2014•2015
FACULTY OF SCIENCES
Master of Statistics

Master's thesis

Longitudinal modeling of T-cell dynamics during in vitro stimulation experiments

Supervisor :
Prof. dr. Niel HENS

Supervisor :
Dr. BENSON OGUNJIMI

Md. Rezaul Karim

Thesis presented in fulfillment of the requirements for the degree of Master of Statistics

Transnational University Limburg is a unique collaboration of two universities in two countries: the University of Hasselt and Maastricht University.

universiteit hasselt
KNOWLEDGE IN ACTION

Universiteit Hasselt | Campus Hasselt | Martelarenlaan 42 | BE-3500 Hasselt
Universiteit Hasselt | Campus Diepenbeek | Agoralaan Gebouw D | BE-3590 Diepenbeek

universiteit hasselt | Maastricht University

2014•2015
FACULTY OF SCIENCES
Master of Statistics

Master's thesis

Longitudinal modeling of T-cell dynamics during in vitro stimulation experiments

Supervisor :
Prof. dr. Niel HENS

Supervisor :
Dr. BENSON OGUNJIMI

Md. Rezaul Karim

Thesis presented in fulfillment of the requirements for the degree of Master of Statistics

universiteit hasselt | Maastricht University

Certification

Thesis submitted in partial fulfillment of the requirements for the degree of Master of Statistics: Biostatistics. I declare that this thesis was written by me under the guidance and counsel of my supervisors.

Student:
Md Rezaul Karim ———————————————— Date: ————————————————
Signature

We certify that this is the true thesis report written by **Md Rezaul Karim** under our supervision and we thus permit its presentation for assessment.

Internal Supervisor:
Prof. Dr. Niel HENS ———————————————— Date: ————————————————
Hasselt University Signature

External Supervisor:
Dr. Benson OGUNJIMI ———————————————— Date: ————————————————
Antwerp University Signature

Acknowledgement

First and foremost I would like to express my sincere gratitude to God for walking with me this far and fulfilling my dreams. He guided, encouraged and always motivated me to soldier on, without which I would never have made it this far. Forever will I be grateful to Him.

I express my sincere gratitude to my favorite teacher and promoter Prof. dr. Niel HENS for giving me the topic of this dissertation. My favorite promoter Prof. dr. Niel HENS was always ready to concentrate my research problems and his invaluable comments and suggestions at different stages of the study have helped me to complete my research work for which I deeply express my thankful gratitude. I am highly grateful to him for allowing me to work under his guidance.

My heartiest gratitude also goes to Dr. Benson OGUNJIMI, Antwerp University, for providing me data and valuable suggestions throughout the research work. I want to express my deep gratitude to all of the respected professors of Center for Statistics, Hasselt University.

I would like to acknowledge the financial support from the Vlaamse Interuniversitaire Raad (VLIR) to fulfill my higher study in Hasselt University. I desire to express my especial thanks to all my fellow colleagues and friends. Around the world we came and in the 2 years, we shared our diverse cultures and bonded into a small global family.

Last but not the least, I am thankful to all the authors from home and abroad whose publications have helped me design my research more scientifically and with strong foundation.

September 1, 2015 Md Rezaul Karim

Longitudinal modeling of T-cell dynamics during in vitro stimulation experiments

Abstract

T-lymphocytes (T-cells) play a vital role in cell-mediated immunity in controlling and eliminating the viral infection. T-cells placed in cell culture can be stimulated using antigen-specific peptides. Upon stimulation, these T-cells will proliferate during cell culture. In vitro stimulation experiment was conducted on 40 patients. The proliferation of T-cells and its dependence on gender, group, CMV status and age were investigated, based on longitudinal measurements of T-cells over time following stimulation of antigen-specific IE62 and IE63 peptides in the different T-cell populations: IFN-γ, IL-2 and both IFN-γ and IL-2. Data were analysed by using a variety of techniques encompassing the analysis of summary statistics, linear mixed models, and latent class linear mixed models. Conclusions were that T-cells proliferated over time following stimulation of IE62 peptides and that males had higher proliferation rate than that of females for all populations. In addition, pediatric nurses group has occupationally a higher proliferation rate than NICU nurse group for both IFN-γ and IL-2 population, whereas there was no effect of group for other two populations. Furthermore, there was no association between T-cells proliferation and CMV status as well as age of the patient. On the other hand, the T-cells increased over time following stimulation of IE63 peptides and there was no significant effect of the group, CMV status and age on this proliferation for all populations. Moreover, the males T-cells proliferation rate was higher than that of the females for only IFN-γ population, but gender had no effect on other two populations.

Keywords: *T-cells, IE62 and IE63, Mixed Models, Latent Class Linear Mixed Models, Sensitivity analysis*

Table of Contents

List of Tables

List of Figures

List of Abbreviations

AIC	Akaike Information Criterion
ANCOVA	Analysis of Covariance
ANOVA	Analysis of Variance
AR(1)	Auto-Regressive of order one
CCMV	Complete Case Missing Value
CMI	Cell-Mediated Immunity
CMV	Cytomegalovirus
EM	Expectation-Maximization
GLM	Generalized Linear Models
HLMM	Heterogeneity Linear Mixed Models
IE62	Intermediate-Early Protein 62
IE63	Intermediate-Early Protein 63
IFN	Interferon
IL	Interleukin
LCMM	Latent Class Linear Mixed Models
LMM	Linear Mixed Models
LR	Likelihood Ratio
MAR	Missing at Random
MCAR	Missing Completely at Random
MHC	Major Histocompatibility Complex
ML	Maximum Likelihoods
MNAR	Missing Not at Random
PHN	Post Herpetic Neuralgia
PMM	Pattern-Mixture Model
Q-Q	Quintile-Quintile
REML	Restricted Maximum Log-Likelihoods
TCR	T-cell Receptor
VZV	Varicella Zoster Virus

1 Introduction

1.1 Background

Varicella zoster virus (VZV) is a common human alphaherpesvirus that responsible for both chickenpox, a result of primary infection, and herpes zoster (shingles), caused by the reactivation of latent virus from neuronal latency in sensory ganglia, generally in the setting of reduced VZV-specific cell-mediated immunity. Herpes zoster may be followed by post herpetic neuralgia (PHN) and other neurologic syndromes (Spengler et al.; 2001; Baiker et al.; 2004; Ogunjimi et al.; 2011; Steain et al.; 2014; Zerboni and Arvin; 2015). The vaccine for chickenpox was developed in 1995, but it is not available in all countries due to its costs (Flatt and Breuer; 2012). The improvement of the VZV vaccine has stimulated new efforts to evaluate cell-mediated immune responses to VZV. The most conventional evaluate of cell-mediated immunity is an antigen stimulation in which lymphocytes from blood are stimulated by an extract of VZV infected cells to proliferate (Hayward; 2001). T-lymphocytes (T-cells) are main actors in cell-mediated immunity in controlling and eliminating the viral infection.

All T-cells come up from haematopoietic stem cells in the bone marrow, but they mature in the thymus. Mature recirculating T-cells that have not yet encountered their antigens are known as naive T-cells. Another type of T-cells that help the action of other immune cells by discharging T-cells cytokines is called helper T-cells (T_h). Mature T_h cells express the surface protein CD4 and that are denoted to as $CD4^+$ T cells. In order for the T-cell receptor (TCR) to attach to the class I major histocompatibility complex (MHC) molecule, the former must be accompanied by a glycoprotein called CD8, which adheres to the fixed portion of the class I MHC molecule. Therefore, these T cells are called $CD8^+$ T cells. Memory T-cell plays a vital role in acquired immune system. According to Lanzavecchia and Sallusto (2000), protective memory is intervened by effector memory T cells (T_{EM}) that transfer to inflamed peripheral tissues and show immediate effector function, whereas reactive memory is intervened by central memory T cells (T_{CM}) that home to T-cell areas of secondary lymphoid organs have little or no effector function, but readily proliferate and differentiate to effector cells in response to antigenic stimulation (Sallusto et al.; 2004; Fiuza et al.; 2009; Belisle et al.; 2011). T-cells placed in cell culture can be stimulated using antigen-specific peptides. Upon stimulation, these different T-cells populations both for CD4 and CD8 T-cells: naive, effector, central memory, and effector memory T-cells will proliferate during culture.

The central memory T-cell produces mainly IL-2 in following TCR triggering but after proliferation they efficiently differentiate to effector cells and produce large amounts of IFN-γ or IL-4. CD8 T_{EM} bring large amounts of perforin, and both CD4 and CD8 produce IFN-γ , IL-4, and IL-5 within hours following antigenic stimulation. The relative proportions of T_{CM} and T_{EM} in blood vary in the CD4 and CD8 compartments; $T_{CM}$is predominant in CD4 and T_{EM} in CD8 (Campbell et al.; 2001).

To explore the impact of exposure to primary Varicella on VZV Immunity, a good number of research and investigations have taken place in many follow-up studies (Arvin et al.; 2001) where it was found that the cellular and humoral responses evolves over time. Ogunjimi et al. (2011) analyzed cellular (IFN-γ ELISPOT) and humoral responses by linear mixed models. They found that the young control group showed higher cellular responses than the older control group. The linear mixed model predicts a decline in cellular response of 50% between 1 week and 1 mo post-exposure, followed by an increase to attain an 80% higher level at 1 year compared to the first week post-exposure. Many studied mentioned a decline in VZV-specific cellular immunity with age (Berger et al.; 1981; Levin et al.; 2003; Miller; 1980). Ogunjimi et al. (2014a) identified a positive association between aging and VZV antibody titers and CMV infection having a negative effect on the number of B-cells while The VZV antibody titer was lower in males than female.

Some studies have investigated several VZV antigens capable of eliciting cellular immune responses (Frey et al.; 2003; Malavige et al.; 2008; Jones et al.; 2007; Ogunjimi et al.; 2014b). It was found both humoral immunity and Cell-mediated immunity (CMI) to VZV intermediate-early protein 63 (IE63) in immune adults and CMI to IE63 remained high in elderly zoster-free individuals (Sadzot-Delvaux and Rentier; 2001). In our study based on vitro stimulation experiment, the antigen-specific peptides VZV intermediate-early protein 62 (IE62) and IE63 were considered to investigate T-cell proliferation for different T-cell populations over time following stimulation of these antigen-specific

peptides.

The report is organized as follows. Section 2 is devoted to the presentation of the methodology of mixed models with a latent class linear mixed models. It is focused on models of interest for analyzing study data. Section 3 provides a specific model for each T-cell population and model based outputs with model diagnostic as well as a sensitivity analysis. A short concluding section summarizes the main points of this report and gives some perspectives for future work.

1.2 Research Objectives

The main objective of this study was to investigate how T-cells proliferate over time following stimulation of antigen-specific IE62 and IE63 peptides in the different T-cell populations: IFN-γ, IL-2 and both IFN-γ and IL-2. And to investigate how these proliferation's depend on baseline correction factors: gender, Cytomegalovirus (CMV) status, group status and age of the patient.

2 Methodology

2.1 Data Descriptions

The data were collected from the blood samples from 40 patients on the initial time (0), 3rd, 7th, and 10th day after applying antigen-specific IE62 and IE63 peptides based on vitro stimulation experiments. For each patient, the identification number, number T-cells after applying antigen-specific IE62 and IE63 peptides, number of cells without stimulus, measurement time since entry into the study (in day), Cytomegalovirus (CMV) status, gender, group status and age at entry into the study (in years) were recorded for each output category (See, details in Table 1).

Table 1: Variable and value description of the study

Variable name	Description
ID	Identification number
$IE62$	Number of T-cells after applying antigen-specific immediate early protein 62
$IE63$	Number of T-cells after applying antigen-specific immediate early protein 63
NEG	Number of cells in 3 wells (750,000 cells) without stimulus
POS	Number of cells in 2 wells (500,000 cells) per stimulus
CMV	Cytomegalovirus (0 = Absent, 1 = Present)
$Gender$	0 = Female, 1 = Male
Age	Age of the patient
$Output$	T-cell Population (1 = Interferon gamma (IFN-γ), 2 = Interleukin (IL)-2, 3 = IFN-γ and IL-2)
$Group$	0 = NICU nurse, 1 = Pediatric nurse
Day	Actual measurement time in Day Time (0, 3, 7, 10)
$Time$	Standardized Time (Time = Day/10)
$LogTime$	Natural logarithm of actual time (LogTime = log(Day))
$SamplingTime$	The time point of sampling in patient allocation
$LastExposureVZV$	The time since last exposure to VZV

The response variables $IE62$ and $IE63$ were modified (defined by $PIE62$ and $PIE63$, respectively) for longitudinal analysis. First, the percentages of antigen-stimulus-induced IFN-γ or/and IL-2-producing T-cell subtypes were calculated per stimulus by subtracting the percentage from the unstimulated samples per stimulus. That is, the percentage of $IE62$ and the percentage of NEG were calculated and the difference between the percentages ($PDIE62$ = Percentage of $IE62$ - Percentage of NEG) were computed. Next, the p-value of Fisher exact test for contingency tables was calculated for assessing whether STIMULUS and NEG were statistically significant. Finally, (i) if p-value $<$ 0.05 and $PDIE62 > 0$, then the $PIE62$ will be an exact value of $PDIE62$. (ii) If p-value > 0.05 or p-value < 0.05 and $PDIE62 < 0$, then we assessed whether the $POS > 100$ or not. If $POS < 100$, then the experiment was not correct and we considered the $PIE62$ as a missing value. If $POS > 100$ we considered $PIE62$ as 0. Similarly, the response variable $PIE63$ was subjected through second and final conditions as done before.

2.2 Data Exploration

As a first step of the analysis, the data were explored in different ways in order to get details that may help to make the decision in the subsequent steps of the analysis. To acquire knowledges about mean and variance structures of the response variables $PIE62$ and $PIE63$ over time, the summary statistics of the $PIE62$ and $PIE63$ in different occasions were tabulated. In order to get an idea about the correlation structure of residuals, the correlation matrix of responses in different occasions was also tabulated. The graphical presentation techniques such as individual profiles plot and mean profile plot were drawn in order to have an idea about the evolution of $PIE62$ and $PIE63$ over time.

2.3 Mixed Model Methodology

2.3.1 Mixed Models

The main objectives of a longitudinal model are the estimation of changes response over time and testing whether these changes are treatment (covariates) dependent (Molenberghs and Verbeke; 2005). That is, the longitudinal models can estimate individual-level (patient-specific) parameters. Special methods of statistical analysis are needed for longitudinal data because the set of measurements on one patient tends to be correlated, measurements on the same patient close in time tend to be more highly correlated than measurements far apart in time, and the variability of longitudinal data often change with time as stated by Verbeke and Molenberghs (2000). These potential patterns of correlation and variation may combine to produce a complicated covariance structure. This covariance structure must be taken into account to draw valid statistical inferences. Therefore, standard regression, Analysis of Variance (ANOVA) and generalized linear models (GLM) may produce invalid results, because two of the parametric assumptions (independent observations and equal variances) may not be valid.

In this study, the comparisons of the T-cells proliferation over time following stimulation of antigen-specific (IE62 and IE63) peptides in the different T-cell populations were done and observations of possible changes between a patient's T-cells proliferation at different time point as well as the correlation between these measurements were accounted for. We build up a mathematical model that fits the evolution profile the best. There are several mathematical models that could be used such as analysis of the area under the curve, analysis of increment, analysis of endpoint, analysis of covariance (ANCOVA) and analysis at each time point, but these methods will lead to substantial loss of information and/ or pose some analytical problems. Multivariate models with general covariance structure are often difficult to apply to highly unbalance data, whereas two-stage model random effects model can be used easily Laird and Ware (1982). The two-stage analysis can still be seen as a case of use of summary statistics, in which the outcome is summarized by the regression coefficients, which are in turn analyzed in the second stage (Verbeke and Molenberghs; 2000). Hence a random-effects model, which combines the two stages, was employed to study the evolutionary difference in the T-cells proliferation of the patients over time.

According to Laird and Ware (1982), random coefficient models are a class of statistical models developed by thinking first about individual "subject-specific" fashion. This model framework is known popularly as the mixed effects model. For continuous responses, the general form of the Mixed Models employed was given by the following

$$\boldsymbol{Y}_i = f(\boldsymbol{X}_i, \boldsymbol{\beta}, \boldsymbol{Z}_i, \boldsymbol{b}_i) + \boldsymbol{\epsilon}_i \tag{2.1}$$

where, $\boldsymbol{Y}_i$ is the vector of response, $\boldsymbol{X}_i$ is the design matrix of fixed effects, $\boldsymbol{Z}_i$ is the design matrix of random effects and $\boldsymbol{\epsilon}_i$ is the vector of residual of ith individual. The vector $\boldsymbol{\beta}$ and $\boldsymbol{b}_i$ are the fixed effects (the predicted variables are supposed to have the same effects for all individuals) and the random effects (the predicted variables also have an additional individual-specific effect, allowing variation between individuals), respectively. The vectors $\boldsymbol{b}_i$ is assumed to be random with normally distributed with zero mean and common covariance matrix $\boldsymbol{D}$ for all patients. Vector $\boldsymbol{\epsilon}_i$ of residual components is usually assumed to be normally distributed with zero mean and covariance matrix Σ_i. Several (linear and non-linear) functional forms f were chosen, such that a wide range of models could be compared. The Akaike Information Criterion (AIC) was used to select the best model among the models under consideration of testing both fixed, and random effects. The restricted maximum log-likelihoods (REML) are used to compare models with the same mean structure while Maximum Likelihoods (ML) are used to compare the models with different mean structures (Verbeke and Molenberghs; 2000). The importance of random effects has been checked by using Likelihood ratio (LR) test and the p-values were calculated by using a mixture of chi-square distribution with equal weight for solving boundary problems of parameter space under the null hypothesis. Both of ML and REML are used in LR test statistic. In fact, the REML test statistic performs slightly better than the ML test statistic in the sense that, on average, the rejection proportions are closer to the nominal level for the REML test statistic than for the ML test statistic (Verbeke and Molenberghs; 2000). We explored various covariance structures to describe the correlation between measurements taken at different time points, ranging from constant to autoregressive (AR(1)) correlation structures.

2.3.2 Latent Class Mixed Models (LCMM)

The linear functional form f of equation (2.1) is well known as a linear mixed model (LMM) for the response vector $\boldsymbol{Y}_i$. The LMM is a special form of random effect models where the normality is assumed for random effects. The regression parameters in LMMs have population averaged interpretations (Fitzmaurice et al.; 2004).

The LMM is written as:

$$\boldsymbol{Y}_i = \boldsymbol{X}_i\boldsymbol{\beta} + \boldsymbol{Z}_i\boldsymbol{b}_i + \boldsymbol{\epsilon}_i \tag{2.2}$$

where $\boldsymbol{X}_i$ is a $n_i \times p$ design matrix for the p vector of fixed effects $\boldsymbol{\beta}$, and $\boldsymbol{Z}_i$ is a $n_i \times q$ design matrix associated to the q vector of random effects $\boldsymbol{b}_i$ which represents the patient-specific regression coefficients. In an homogeneous mixed model like equation (2.2), $\boldsymbol{b}_i$ is normally distributed with mean $\boldsymbol{\mu}$ and covariance matrix $\boldsymbol{D}$ i.e. $\boldsymbol{b}_i \sim N(\boldsymbol{\mu}, \boldsymbol{D})$.

The assumption of normal distribution of random effects $\boldsymbol{b}_i$ of homogeneous mixed model (2.2) can be then violated and rather a mixture of two or more normals should be considered as a distribution of random effects $\boldsymbol{b}_i$. The heterogeneity linear mixed model (HLMM) that was proposed by Verbeke and Lesaffre (1996) and also described by Verbeke and Molenberghs (2000) is obtained by replacing this distributional assumption by a mixture of a prespecified number g of normal distributions with mean vectors μ_k and covariance matrices D, i.e.

$$\boldsymbol{b}_i \sim \sum_{k=1}^{g} \pi_k N(\boldsymbol{\mu}_k, \boldsymbol{D}) \tag{2.3}$$

with $0 \leq \pi_k \leq 1$, $\sum_{k=1}^{g} \pi_k = 1$ and $\boldsymbol{\mu}_k = (\mu_0^k, \mu_1^k, ..., \mu_g^k)^t$ rather than from just one single normal distribution with $N(\boldsymbol{\mu}, D)$. This not only extends the assumption about the random-effects distribution to a very broad class of distributions (unimodal as well as multimodal, symmetric as well as highly skewed), it is also perfectly suitable for classification purposes, based on longitudinal profiles. Under the assumption (2.3), Proust and Jacqmin-Gadda (2005) proposed a slightly more general formulation of the model described in (2.2) in which the effect of some covariates may depend on the components of mixture and some of the random effects may have a common mean whatever the component of mixture. Thus, the $\boldsymbol{X}_i$ design matrix is split in $\boldsymbol{X}_{1i}$ associated with the vector $\boldsymbol{\beta}$ of fixed effects which are common to all the components and $\boldsymbol{X}_{2i}$ associated with the vectors $\boldsymbol{\delta}_k$ of fixed effects which are specific to the components. The $\boldsymbol{Z}_i$ design matrix is also splitted in $\boldsymbol{Z}_{1i}$ associated with the vector $\boldsymbol{b}_{1i}$ of random effects following a single Gaussian distribution and $\boldsymbol{Z}_{2i}$ associated with the vector $\boldsymbol{b}_{2i}$ of random effects following a mixture of Gaussian distributions.

The model is then written as:

$$\boldsymbol{Y}_i = \boldsymbol{X}_{1i}\boldsymbol{\beta} + \sum_{k=1}^{g} \pi_k \boldsymbol{X}_{2i}\boldsymbol{\delta}_k + \boldsymbol{Z}_{1i}\boldsymbol{b}_{1i} + \boldsymbol{Z}_{2i}\boldsymbol{b}_{2i} + \boldsymbol{\epsilon}_i \tag{2.4}$$

where $\boldsymbol{b}_{1i} \sim N(\boldsymbol{0}, \boldsymbol{D}_{b_1})$ and $\boldsymbol{b}_{2i} \sim \sum_{k=1}^{g} \pi_k N(\boldsymbol{\mu}_k, \boldsymbol{D}_{b_2})$ given the component k, the conditional distribution of the vector

$$\boldsymbol{b}_i = \begin{pmatrix} \boldsymbol{b}_{1i} \\ \boldsymbol{b}_{2i} \end{pmatrix} \sim N\left(\begin{pmatrix} \boldsymbol{0} \\ \boldsymbol{\mu}_k \end{pmatrix}, \boldsymbol{D} \right) \quad with \quad \boldsymbol{D} = \begin{bmatrix} \boldsymbol{D}_{b_1} & \boldsymbol{D}_{b_1 b_2} \\ \boldsymbol{D}_{b_2 b_1} & \boldsymbol{D}_{b_2} \end{bmatrix}.$$

The model (2.4) is called a Latent Class Linear Mixed Models (LCMM) and it is also called finite mixture mixed model with assuming that the population is heterogeneous and constituted of g latent classes of patients characterized by g mean profiles of trajectories (Proust and Jacqmin-Gadda; 2005; Proust-Lima et al.; 2015; Muthén and Shedden; 1999; Celeux et al.; 2002).

Each patient belongs to one and only one latent class (mixture component) so that the latent class membership is defined by a discrete random variable c_i that equals k if patient i belongs to latent class $k(k = 1, ..., g)$. The variable c_i is latent; its probability is described using a multinomial logistic model according to covariates X_{ci}:

$$\pi_{ik} = P(c_i = k|X_{ci}) = \frac{e^{\xi_{0k}+X_{ci}^T\xi_{1k}}}{\sum_{k=1}^{g} e^{\xi_{0k}+X_{ci}^T\xi_{1k}}} \tag{2.5}$$

where ξ_{0k} is the intercept for class k and ξ_{1k} is the q_1-vector of class-specific parameters associated with the q_1-vector of time-independent covariates X_{ci}. The g mean profiles are defined according to time and covariates through latent class specific mixed models. The difference with a standard linear mixed model is that both fixed effects and the distribution of the random-effects can be class-specific (Proust-Lima et al.; 2015).

The Expectation-Maximization (EM) algorithm is used to estimate the parameters of the LCMM. The initial values for EM algorithm are chosen from the estimates of standard LMM. The patient will be classified based on posterior probabilities such that classifies the ith patient into the component for which it has the highest estimated posterior probability. Further discussion and estimation with classification about LCMM can be found in Muthén and Shedden (1999); Lenk and DeSarbo (2000); Verbeke and Molenberghs (2000); Proust-Lima et al. (2015).

2.3.3 Model Diagnostics

After fitting a statistical model, it is important to determine whether all the necessary model assumptions are valid before performing inference. If there are any violations, subsequent inferential procedures may be invalid, resulting in faulty conclusions. Therefore, it is crucial to perform appropriate model diagnostics. The histograms and/or Quintile-Quintile (Q-Q) plot with Shapiro-Wilk test are used to check the normality assumption of random effect $\boldsymbol{b}_i$, although these plots of the predicted random errors for the purpose of checking their normality are of limited value. That is because the observed distribution of $\widehat{\boldsymbol{b}_i}$, does not necessarily reflect the true distribution of $\boldsymbol{b}_i$ because of its shrinkage estimates. It is worth noting, however, that if the inferential goal focuses on the marginal model (2.1), and especially on the fixed effects $\boldsymbol{\beta}$, valid inference can be obtained even if the random effects do not follow a normal distribution (Verbeke and Molenberghs; 2000). Gałecki and Burzykowski (2013) mentioned using histogram or Q-Q plot of the transformed raw conditional or marginal residuals by applying Cholesky decomposition to check the normality of residual assumption. The normal Q-Q plot of this transformed residuals should show approximately a straight line. In case of non-normality of measurement error, the log transformation and/or Box-Cox power transformation will be performed. If there is a not a good fit of the mixed model to the data, then determining which profiles are outlying is a risky activity and should be used with caution.

Diagnostic methods to detect outliers and influential points have been proposed in LMM, but they are not well developed for all types of mixed model. The need for better or more utilized diagnostics for models with random effects and/or correlated errors has been noted by a number of authors, including, Verbeke and Molenberghs (2000); Tan et al. (2001); Houseman et al. (2004); Jensen et al. (2006); Gałecki and Burzykowski (2013). However, in this study, local influence approach and global measure are used to detect outliers and/or influential.

2.4 Sensitivity Analysis

The longitudinal data at hand contained some missing values. To obtain valid inferences from partially missing longitudinal data, the nature of the missing data mechanism must be considered. Little and Rubin (1989) introduced a formal framework for the field of incomplete data by introducing the important taxonomy of missing data mechanisms, consisting of missing completely at random (MCAR), missing at random (MAR), and missing not at random (MNAR). The MCAR mechanism potentially depends on observed covariates, but not on observed or unobserved outcomes. The essential feature of MCAR is that the observed data can be thought of as a random sample of the complete data. This implies that with data MCAR it is legitimate, but possibly wasteful, to remove patients with any missing data from the analysis since they can be regarded as randomly chosen without regard to their data values. The MAR mechanism depends on the observed outcomes and perhaps also on the covariates, but not further on unobserved measurements. With MAR, the observed data cannot be viewed as a random sample of the complete data, which leads to important implications for analyzing. Finally, when a MNAR mechanism is operating, missingness does depend on

unobserved measurements, perhaps in addition to dependencies on covariates and/or on observed outcomes. Under MNAR mechanism, the probability that responses are missing is related to the specific values that should have been obtained. Therefore, under MNAR, missingness cannot be ignored (Fitzmaurice et al.; 2004; Molenberghs and Kenward; 2007).

In practice, the reasons for missingness are likely to be many and varied, and it is, therefore, difficult to justify solely on a priori grounds the assumption of missingness at random. Indeed, patients often leave the study prematurely for reasons related to the outcome of interest, rendering MCAR less plausible as a mechanism and suggesting that MAR, or perhaps even MNAR, ought to be explored. Arguably, under MNAR, a wholly satisfactory analysis of the data is not feasible, and it should be noted that the data alone cannot distinguish between MAR and MNAR mechanisms (Molenberghs and Kenward; 2007). It is, therefore, desirable to check the sensitivity of the conclusion to unverifiable assumptions. In this study, a simple sensitivity analysis for the LMM for the Gaussian case was performed under pattern-mixture family by conducting an analysis by pattern, such that a separate analysis is obtained for each of the dropout patterns (Verbeke and Molenberghs; 2000). Besides, sensitivity based on multiple imputations is carried out by application of shift and inflation factor to imputed data (Molenberghs and Verbeke; 2005; Yuan; 2014). This procedure is used as a stress test to investigate how sensitive the conclusions are to deviations from multiple imputations in its basic form under MAR.

2.5 Statistical Computation

All statistical analysis were performed in R (version 3.2.0) software by using lcmm, sp, CAMAN, mi, mice, mitools and lattice packages and SAS software version 9.4 by using proc mixed, mi and mianalyze.

This page intentionally left blank

3 Results

3.1 Data Exploration

A total of 40 patients were involved in the study and the data were balance in terms of the prognostic factors $group$ (50% patients for pediatric nurse group) and CMV status (50% patients were CMV positive) but it was highly unbalanced in terms of $gender$ that only 6 (15%) patients were male and remaining 34 (85%) patients were female. The age of the patients at entry in the study ranges from 22 to 53 years and the average age was 39.03 years. The data were found to be unbalanced with measurements taken at four fixed time points and not all scheduled measurements were available, for unknown reason.

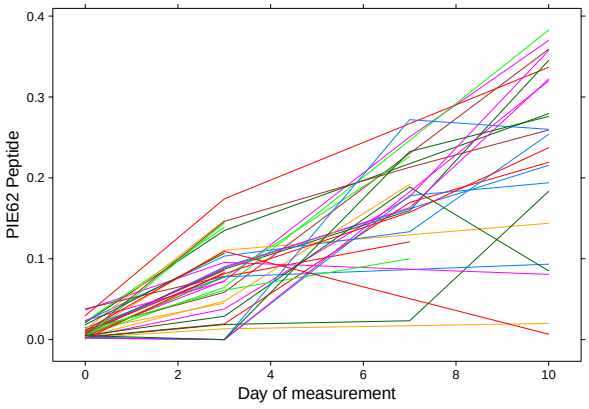

Figure 1: Individual profile plots of PIE62 for IFN-γ

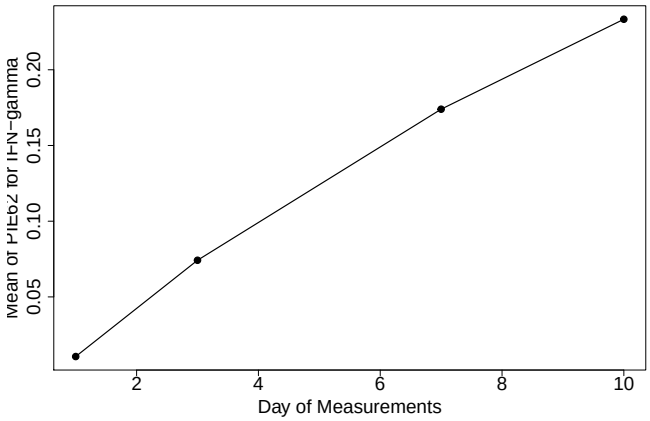

Figure 2: Mean Structure of PIE62 for IFN-γ

The individual and mean of $PIE62$ profile plots of all patients over measurement day for IFN-γ population are depicted in Figure 1 and Figure 2, respectively. It is observed that the patients had different starting $PIE62$ scores with a lot of between and within patients variability which gives an indication for fitting a mixed model. From mean plot, it seems to be a linear evolution of $PIE62$ over time while individual profile plot shows that a few patients had a curvature evolution over time. The summary statistics of $PIE62$ and $PIE63$ are tabulated in Table 2. It is noticed that the variability of $PIE62$ increased over time with increasing average score.

The individual profile and mean plots of $PIE62$ for IL-2 population are plotted in Figure A1 and Figure A2, respectively. These plots show a huge between and within patients variability of $PIE62$ and curvature average evaluation over time. The $PIE62$ score of some patients sharply increased and some declined after 7th day, which may be due to the effect of the prognostic factor(s). From Table 2 and mean plot, it is clearly shown that the average $PIE62$ decreased in the 3rd day and then rapidly increased up to 7th day and finally slightly increased to 10th day which indicates there was a polynomial $time$ effect on evolution. The Figure A3 and Figure A4 display the individual and mean profiles of $PIE62$ for both IFN-γ and IL-2 population. It is noticed that a large between and within variation of $PIE62$ scores and the mean profile increased over time with curvature evolution. The correlations of responses between time points are tabulated in Table A1. It is worth noting that the correlation decreases for measurements obtained at more distant timepoints and a few correlations were significant which is a very strange behavior for longitudinal settings.

The individual profiles of $PIE63$ for IFN-γ, IL-2 and both IFN-γ and IL-2 populations are exhibited in Figure 3, Figure A5 and Figure A7, respectively. All figures show a lot of within and between variability of patients. It is clearly shown that the $PIE63$ score rapidly increased after the 7th day for some patients and a few patient's PIE63 score rapidly decreased in that time, which seem to indicate that the patients selected from different (mixture) populations. It is also noticed that the score of $PIE63$ of some patients for both IFN-γ and IL-2 population seems to be

Table 2: The summary statistics mean (standard deviation) of PIE62 and PIE63 responses

	PIE62			
T-cell Population	Day 0	Day 3	Day 7	Day 10
IFN-γ	0.0106(0.0095)	0.0742(0.0457)	0.1740(0.0597)	0.2334(0.1125)
IL-2	0.0068(0.0062)	0.0047(0.0041)	0.0412(0.0394)	0.0482(0.0024)
IFN-γ and IL-2	0.0024(0.0014)	0.0017(0.0010)	0.0073(0.0059)	0.0127(0.0128)
	PIE63			
IFN-γ	0.0053(0.0046)	0.0174(0.0192)	0.1289(0.0723)	0.1406(0.0990)
IL-2	0.0043(0.0036)	0.0017(0.0023)	0.0178(0.0315)	0.0300(0.0446)
IFN-γ and IL-2	0.0016(0.0007)	0.0009(0.0008)	0.0076(0.0106)	0.0103(0.0123)

constant over time, which indicates, the evolution of those patients might not depend on time as well as covariates.

The mean profiles of $PIE63$ for IFN-γ, IL-2 and both IFN-γ and IL-2 population are presented in Figure 4, Figure A6 and Figure A8, respectively. All mean plots indicate the curvature evolution of $PIE63$ over time. The correlations of between responses in different time points are tabulated in Table A2. It is very strange that some non-significant correlations between measurements for IL-2 and both IFN-γ and IL-2 population are observed. This might be due to the non-linear relationship between measurements in the same patients.

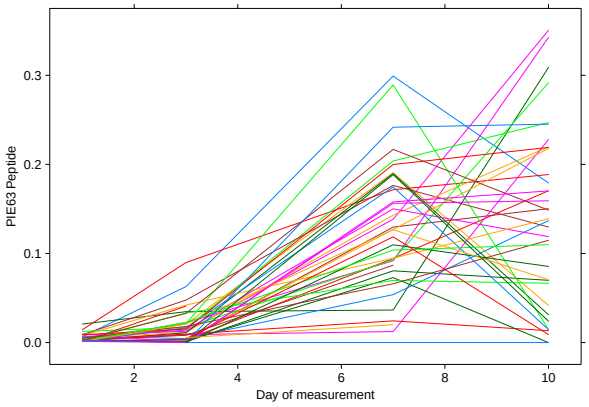

Figure 3: Individual profile plots of PIE63 for IFN-γ

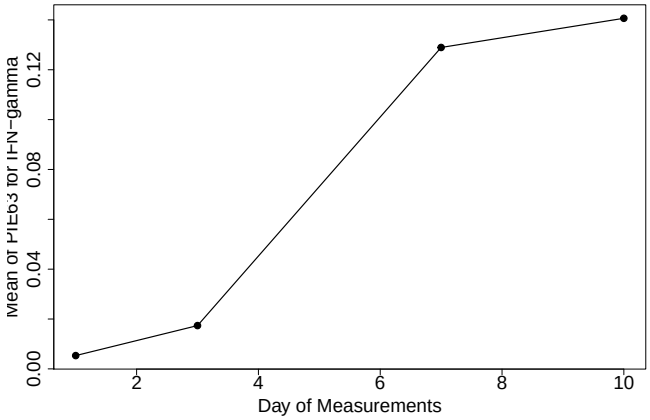

Figure 4: Mean Structure of PIE63 for IFN-γ

Figure A9 to Figure A20 investigated the possible effect of $group$ and CMV status and their two-way interactions with time. Some average evolution's are parallel and some are crossed initially and then again crossed later. These graphs indicate the $group$ and CMV status might not be significant on the evolution of $PIE62$ and/or $PIE63$ in each $output$ category. Similar plots (not displayed in the report) were drawn for $gender$ and observed that $gender$ seems to have an effect on evolution of $PIE62$ in each population. The $gender$ also seems to have an effect on evolution of $PIE63$ only for INF$-\gamma$ population. However, $gender$ seems not to have a significant on evolution of $PIE63$ for IL-2 and both IFN-γ and IL-2 populations.

We also investigated the bivariate association by using chi-square and Fisher exact tests between categorical covariates which might be helpful in investigating multicollinearity in the model. The results are provided in the Table A3. It is revealed that there was no association between covariates $gender$, $group$ and CMV status at 5% level of significance.

3.2 Modeling of PIE62 for Different T-cell Populations

3.2.1 Modeling of PIE62 for IFN-γ Population

The linear (in parameter) functional form of mixed model (2.1) with all possible two-way interaction between time and covariates was initially considered. In order to confirm whether a linear effect of time is sufficient to describe the evolution, a quadratic effect time was fitted and then tested via F-test. The result confirmed only the linear effect was significant and quadratic effect was not significant (F-test = 0.41, p-value = 0.5266). Moreover, a significant dependence of the evolution of the $PIE62$ on an interaction between $gender$ and $time$ was also observed but other interactions were not significant. Therefore, the interaction between $gender$ and $time$ was considered in model (3.1) with the main effect of other covariates, although they were not significant, but they might be important for the interpretation in biological point of view. Both random intercept and slope were included in the model to capture within-patient variability. The p-value of Restricted Maximum Likelihood Ratio (REML) test, shown on Table 3, which is calculated by using a mixture of chi-square ($\chi^2_{1:2}$) with equal weight and random slopes were found to be significant (LR test statistic = 41.0 and p-value = <0.001). It can be concluded that the random slopes have to be kept in the final model. Therefore, the final model is following:

$$PIE62_{ij} = \beta_0 + b_{0i} + (\beta_1 + b_{1i})Time_{ij} + (\beta_2 + \beta_3 Time_{ij})Gender_i + \beta_4 Group_i + \beta_5 CMV_i + \beta_6 Age_i + \epsilon_{ij} \quad (3.1)$$

where b_{0i} and b_{1i} are patient-specific intercept and slope, respectively for patient i. The random effects are assumed to be independent with $\boldsymbol{b}_i = (b_{0i}, b_{1i})^t \sim N(0, D)$. The ϵ_{ij} is the measurement error with AR(1) correlation structure. The parameter estimates are presented in Table 3 which showed the positive evolution over time and female's PIE62 score decreased over time compared to male's (reference category). It was mentioned earlier that the covariates: $group$, CMV, and age were not significant on the evolution of $PIE62$.

Table 3: REML estimates under hierarchical interpretation of model (3.1), as well as under H_0 (of no random slopes)

		$d_{ii} \geq 0, \sigma^2 \geq 0$			Under $H_0 : d_{12} = d_{21} = d_{22} = 0, \sigma^2 \geq 0$		
Effect	**Parameter**	**Estimate**	**St. Error**	$P-$**value**	**Estimate**	**St. Error**	$P-$**value**
Intercept	β_0	-0.0103	0.0199	0.6091	-0.0229	0.0331	0.4936
Time	β_1	0.3337	0.0567	<0.0001	0.3333	0.0406	<0.0001
Gender	β_2	0.0202	0.0147	0.1768	0.0160	0.0247	0.5176
Gender×Time	β_3	-0.1238	0.0605	0.0473	-0.1232	0.0436	0.0061
Group	β_4	-0.0125	0.0079	0.1226	-0.0121	0.0129	0.3531
CMV	β_5	-0.0050	0.0078	0.5210	0.0047	0.0128	0.7158
Age	β_6	0.0003	0.0004	0.5149	0.0006	0.0007	0.4059
var(b_{0i})	d_{11}	6.53×10^{-5}	–	–	0.0001	–	–
cov(b_{0i}, b_{1i})	$d_{12} = d_{21}$	-0.0010	–	–	–	–	–
var(b_{1i})	d_{22}	0.0095	–	–	–	–	–
AR(1)	ρ	-0.0982	–	–	0.2260	–	–
Residual var.	σ^2	0.0015	–	–	0.0035	–	–
-2×REML		-332.80			-289.80		

In addition, to get more insight about the effect of covariates on evolution, complete case missing value (CCMV) restrictions of the LMM under different dropout patterns were performed. The results are displayed in Table A4. Under pattern 1 (i.e. complete case up to day 7), the main effect of $time$ and $group$ are found to be significant. Under pattern 2 (i.e. complete case up to day 10), it is apparent that the parameter estimates of the main effect of $time$ and interaction between $time$ and $gender$ were significant, while $group$ was not significant and conclusions are similar to main analysis showed in Table 3.

3.2.1.1 Model Diagnostics

The model diagnostic plots are shown in Figure A21. It is shown that the histogram and Q-Q plot of patient-specific residual follow a normal distribution and the random slope (Shapiro-Wilk normality test: $p-$value = 0.405) also follow a normal distribution. However, the Empirical Bayes estimates of random effects may suffer from the effect of shrinkage. The predicted individual and mean profile are displayed in Figure A22 and Figure A23, respectively. These plots are similar to observed individual and mean plots which indicates model 3 is good for prediction.

3.2.1.2 Sensitivity Analysis

The analyzes in the previous subsections were conducted based on the direct likelihood approach which is valid provided the missing data mechanism are MAR and under some mild regularity conditions (Molenberghs and Kenward; 2007). To explore the impact of deviations from the assumption of MAR, the LMM was considered under two different scenarios, based on the pattern-mixture model (PMM) approach to multiple imputation under the MNAR assumption by using specified shift parameters (0.10 and 0.20) to adjust imputed $PIE62$. The results of mentioned analysis are presented in Table 4. The parameter estimates under MNAR with various scenarios and under MAR are quite similar. Therefore, given that there is not a big difference across the parameter estimates and their the standard errors, the assumption of MAR seems to hold, although the acceptance of this assumption should be looked with caution since it is untestable.

Table 4: Sensitivity analysis of LMM (3.1) under different scenarios by using multiple imputation (imputed 10 data sets)

		PMM under MNAR			
		Shift = 0.10		Shift = 0.20	
Effect	Parameter	Estimate	Std. Error	Estimate	Std. Error
Intercept	β_0	-0.0409	0.0397	-0.0102	0.0369
Time	β_1	0.3602	0.0445	0.3574	0.0585
Gender	β_2	0.0206	0.0195	0.0284	0.0263
Gender×Time	β_3	-0.1132	0.0484	-0.0327	0.0650
Group	β_4	-0.0134	0.0131	-0.0109	0.0163
CMV	β_5	-0.0067	0.0174	-0.0232	0.0155
Age	β_6	0.0006	0.0010	0.0002	0.0009

3.2.2 Modeling of PIE62 for IL-2 Population

The exploratory analysis indicated a lot of between and within variability among measurements. In order to account these variabilities among measurements, random-effects model (2.1) was considered. Marginal Restricted Maximum log-likelihood ratio test was conducted to investigate the importance of the random slopes for both linear and quadratic time effect in the model. It is observed that in both cases, the p-value less than 0.001 and concluded that the random slopes for linear and quadratic time effect were kept in the final model. All possible two-way interactions except interaction between $gender$ and $time$ found insignificant at 5% level of significance. Therefore, the only interaction between $gender$ and $time$ were retained in the final model with the main effect of other covariates, although they were not significant, but they might be important for the interpretation in biological point of view. The following model (3.2) is considered as a final model.

$$PIE62_{ij} = \beta_0 + b_{0i} + (\beta_1 + b_{1i})Time_{ij} + (\beta_2 + b_{2i})Time_{ij}^2 + \beta_3 Time_{ij}^3 + (\beta_4 + \beta_5 Time_{ij})Gender_i + \beta_6 Group_i + \beta_7 CMV_i + \beta_8 Age_i + \epsilon_{ij} \quad (3.2)$$

where b_{0i}, b_{1i} and b_{2i} are patient-specific intercept, slopes for linear and cubic, respectively and ϵ_{ij} is the measurement error with AR(1) correlation structure. The random effects are assumed to be independent with $\boldsymbol{b}_i = (b_{0i}, b_{1i}, b_{2i})^t \sim$

$N(0, D)$. The parameter estimates of the random-effects model are provided in Table 5. It is observed that the estimates of quadratic and cubic time and the main effect of $gender$ with the interaction between $gender$ and $time$ were highly significant. It was mentioned earlier that other covariates: $group$, CMV status and age were not found significant on the evolution of $PIE62$ for IL-2 T-cell population.

Table 5: REML estimates under hierarchical interpretation of model (3.2), as well as under H_0 (of no random slope for Time^2)

		$d_{ii} \geq 0, \sigma^2 \geq 0$			Under $H_0 : d_{13} = d_{23} = d_{33} = 0$		
Effect	**Parameter**	**Estimate**	**St. Error**	$P-$**value**	**Estimate**	**St. Error**	$P-$**value**
Intercept	β_0	0.0026	0.0049	0.5957	0.0005	0.0065	0.9449
Time	β_1	-0.0524	0.0411	0.2108	-0.0516	0.0442	0.2504
Time^2	β_2	0.3977	0.0915	0.0001	0.4059	0.1003	0.0001
Time^3	β_3	-0.2493	0.0605	0.0003	-0.2553	0.0666	0.0003
Gender	β_4	0.0092	0.0040	0.0286	0.0117	0.0051	0.0252
Gender$\times$Time	β_5	-0.0626	0.0242	0.0153	-0.0660	0.0261	0.0141
Group	β_6	-0.0019	0.0016	0.2331	-0.0026	0.0022	0.2560
CMV	β_7	-0.0014	0.0015	0.3596	-0.0031	0.0022	0.1618
Age	β_8	0.0001	0.0001	0.6250	0.0001	0.0001	0.9439
var(b_{0i})	d_{11}	2.40×10^{-5}	–	–	2.36×10^{-5}	–	–
cov(b_{0i}, b_{1i})	$d_{12} = d_{21}$	-0.0004	–	–	-0.0003	–	–
var(b_{1i})	d_{22}	0.0059	–	–	0.0024	–	–
cov(b_{0i}, b_{2i})	$d_{13} = d_{31}$	0.0002		–	–	–	–
var(b_{2i})	d_{33}	-0.0043	–	–	–	–	–
AR(1)	ρ	-0.5655	–	–	-0.4331	–	–
Residual	σ^2	0.0002	–		0.0003	–	–
-2 $\times$REML		-649.3			-628.0		

3.2.2.1 Model Diagnostic

The model diagnostics plots are depicted in Figure A24 and Q-Q plot and histogram of patient-specific residuals indicate the assumption of normality is satisfied. The residual plot showed two outliers measurements (came from the same patient or different patients). The global influence (restricted likelihood distance) plot showed only a patient (ID = 7) was outlier and highly influence the value of restricted maximum likelihood. This plot is presented in Figure A25. The local influence (deletion estimates) plot also shows that this patient influenced the fixed effect of quadratic and cubic time. However, the conclusions about the significance or importance of covariates were still remained same without and with this patient. The local plots are not displayed in this report. The predicted individual and mean plots are displayed in Figure A26 and Figure A27, respectively. These plots indicate that the model is good for predicting the observed value. The correlation between observed and predicted $PIE62$ is 0.93 which indicates high association between observed and predicted $PIE62$.

3.2.2.2 Sensitivity Analysis

To assess the stability of conclusions under the assumption of MAR, sensitivity analysis was performed under different scenarios, based on the PMM approach to multiple imputations under the MNAR assumption by using specified shift parameter (0.10 and 0.20) to adjust imputed $PIE62$. After using imputed values, the parameter estimates are presented in A5. It is observed that the parameter estimate under MNAR with various scenarios and under MAR are similar. Therefore, given that there is not a big difference across the parameter estimates and the standard errors, the assumption of MAR seems to hold and the conclusions are stable from the deviation of MAR assumption.

3.2.3 Modeling of PIE62 for both IFN-γ and IL-2 Population

Different functional forms of f of the mixed model (2.1) with all possible two-way interaction between time and covariates were considered initially. In assessing the possibility of reducing the number of random effects at a linear and quadratic time, marginal testing for the need of random effects under hierarchical interpretation was used. Based on observed significance level (p-value) for fixed effects and random effects as well as minimum AIC, model (3.3) was chosen. The parameter estimates of this model with -2 $\times$ REML are tabulated in Table 6. The random slopes for a linear and quadratic time effect are tested (in both cases, p-value < 0.001) and found to be significant at 5% level. Therefore, both random slopes were kept in the final model.

The final model is of the form:

$$PIE62_{ij} = \beta_0 + b_{0i} + (\beta_1 + b_{1i})Time_{ij} + (\beta_2 + b_{2i})Time_{ij}^2 + \beta_3 Gender_i + \beta_4 Gender_i \times Time_{ij}^2 + \beta_5 Group_i + \beta_6 CMV_i + \beta_7 Age_i + \epsilon_{ij} \quad (3.3)$$

where b_{0i}, b_{1i} and b_{2i} are patient-specific intercept, linear and quadratic evolution over time, respectively and ϵ_{ij} is the measurement error with AR (1) correlation structure. The random effects are assumed to be independent with $\boldsymbol{b}_i = (b_{0i}, b_{1i}, b_{2i})^t \sim N(0, D)$. It was observed that the interaction between $gender$ and $time$ was significant in the random effect model under H_0 whereas the $p-$value for this interaction in the final model (under H_1) was on a borderline situation. It might be due to unbalanced patient allocation for $gender$, which was mentioned in data exploration in Section 3.1. Therefore, the interaction between $gender$ and $time$ was kept in the final model. The estimated coefficient of $group$ was negative, which was significant on the evolution of $PIE62$. It indicates that patients under supervision of NICU nurses group (0) had a less $PIE62$ score than the patients under supervision of pediatric nurse group (1).

Table 6: REML estimates under hierarchical interpretation of model (3.3), as well as under H_0 (of no random slope for Time^2)

		$d_{ii} \geq 0, \sigma^2 \geq 0$			Under $H_0 : d_{13} = d_{23} = d_{33} = 0, \sigma^2 \geq 0$		
Effect	**Parameter**	**Estimate**	**St. Error**	$P-$**value**	**Estimate**	**St. Error**	$P-$**value**
Intercept	β_0	0.0021	0.0008	0.0164	0.0013	0.0013	0.3363
Time	β_1	-0.0053	0.0040	0.1929	-0.0053	0.0047	0.2703
Time^2	β_2	0.0261	0.0071	0.0014	0.0270	0.0067	0.0003
Gender	β_3	0.0018	0.0006	0.0080	0.0034	0.0010	0.0015
Time$^2\times$Gender	β_4	-0.0114	0.0057	0.0711	-0.0135	0.0061	0.0356
Group	β_5	-0.0014	0.0004	0.0032	-0.0017	0.0004	0.0002
CMV	β_6	-0.0002	0.0003	0.5565	0.0002	0.0004	0.5860
Age	β_7	0.0001	0.0001	0.2966	0.0001	0.0001	0.0824
var(b_{0i})	d_{11}	1.46 $\times 10^{-6}$	–	–	3.52 $\times 10^{-6}$	–	–
cov(b_{0i}, b_{1i})	$d_{12} = d_{21}$	-0.00002	–	–	-0.00001	–	–
var(b_{1i})	d_{22}	0.00032	–	–	0.0002	–	–
cov(b_{0i}, b_{2i})	$d_{13} = d_{31}$	0.00003	–	–	–	–	–
cov(b_{2i}, b_{1i})	$d_{23} = d_{32}$	-0.00041	–	–	–	–	–
var(b_{2i})	d_{33}	0.00061		–	–	–	–
AR(1)	ρ	-0.6213	–	–	-0.1323	–	–
Residual	σ^2	6.46$\times 10^6$	–	–	0.000019	–	–
-2$\times$REML		-718.10			-691.40		

3.2.3.1 Model Diagnostic

Model diagnostics plots are presented in Figure A28. The Q-Q plot and histogram of subject-specific residuals indicate the assumption of normality is satisfied. The predicted individual and mean profile are displayed in Figure A29 and

Figure A30, respectively. These plots indicate the model is good for predicting the observed values. The correlation between observed and predicted $PIE62$ is 0.965 which indicates the high linear relationship between observed and predicted values.

3.2.3.2 Sensitivity Analysis

The analyses and results presented in Table 6 were conducted based on the direct likelihood approach under the assumption of MAR. This assumption cannot be verified, because the missing values were not observed (Schafer; 1997). It is important to examine the sensitivity of inferences to departures from the MAR assumption. To explore the MAR assumption, LMM was performed under two different scenarios, based on the PMM approach to multiple imputations under the MNAR assumption by using specified shift parameter (0.10 and 0.20) to adjust imputed $PIE62$. After using imputed values, the parameter estimates were presented in Table A6. It can be seen that the parameter estimates under various MNAR scenarios and under MAR are not similar. Therefore, given that there is a big difference across the parameter estimates and their standard errors, it means is that, when changing assumptions about the missing data mechanism, data analysis conclusions change. It establishes that there is a certain amount of sensitivity. Therefore, the estimated results should be interpreted with cautions.

3.3 Modeling of PIE63 for Different T-cell Populations

3.3.1 Modeling of PIE63 for IFN-γ Population

At first, we considered different forms of f of model (2.1) and performed the test of the importance of random effects with checking the goodness-of-fits. It was observed, the mixture within $PIE63$ had not been captured by existing covariates with their possible two-way interactions. It was mentioned in exploratory data analysis that the profiles looked like some clusters. Summaries of different model comparisons statistics are presented in Table A7. Based on model comparison criteria, finally a latent class linear mixed model (mixture mixed model) (2.4) of the response variable $PIE63$ for IFN-γ population was considered for modeling. To check the significance of random slopes, Maximum Likelihood Ratio (MLE) tests, shown on Table 7 were conducted and the p-values were calculated by using a mixture of chi-square distribution with equal weight. Patient specific random slope for a linear and quadratic time were found to be significant (in both cases, p-value = <0.001). Random slopes were kept in the final model due to its significant effect. Therefore, the final model (3.4) for kth latent class was fitted with $g = 2$ mixture components is specified as:

$$PIE63_{ij} = \beta_0 + b_{0i} + (\beta_1^k + b_{1i})Time_{ij} + (\beta_2^k + b_{2i})Time_{ij}^2 + \beta_3^k Time_{ij}^3 + \beta_4 Gender_i + \beta_5 Gender_i \times Time_{ij} + \beta_6 Group_i + \beta_7 CMV_i + \beta_8 Age_i + \epsilon_{ij} \quad (3.4)$$

where $\boldsymbol{\beta} = (\beta_0, \beta_4, \beta_5, \beta_6, \beta_7, \beta_8)^t$ is the vector of overall fixed effects and $\boldsymbol{\delta}_k = (\beta_1^k, \beta_2^k, \beta_3^k,)^t$ is the kth class specific fixed effects. The $\boldsymbol{b}_{1i} = b_{0i}$ and $\boldsymbol{b}_{2i} = (b_{1i}, b_{2i})^t$ are the vector of patient specific random effects.

The random effect $\boldsymbol{b}_{1i} \sim N(0, \boldsymbol{D}_{b_1})$ and $\boldsymbol{b}_{2i}$ is now assumed to follow a mixture of two normal distributions with common covariance matrix D_{b_2}, i.e. $\boldsymbol{b}_{2i} \sim \sum_{k=1}^{g=2} \pi_k N(\boldsymbol{\mu}_k, \boldsymbol{D}_{b_2})$ with $\boldsymbol{\mu}_k = (\mu_1^k, \mu_2^k)^t$. The vectors $\boldsymbol{b}_i$, $i = 1, ..., 40$ are assumed to be independent. All error components ϵ_{ij} are considered to be independent and normally distributed with mean zero and common variance σ^2. Parameter estimates are presented in the Table 7. It is observed that $group$, CMV and age were not significant while the interaction between $gender$ and $time$ was significant. It is also seen that the average males $PIE63$ score increased over time compared to that of females (reference category).

Based on posterior probabilities obtained by equation (2.5), patients are classified into two mixture classes. It is noticed that mixture class 1 contained 60% ($\pi_1 = 0.60$) and class 2 contained 40% ($\pi_2 = 0.40$) patients. Patient distribution of different latent classes is presented in Table 8. To get more insight about the reasons of this mixture, the association between latent class variable (C_i) and *sampling time* as well as *last exposure to VZV* were investigated. The results are presented in Table A11. The results indicate that there was a strong association (chi-square = 10.86, p-value = 0.029) between C_i and *sampling time*. It also shows that there was a strong association ($\eta = 0.52$) between C_i and *last exposure to VZV*. Both variables shared 27% (= η^2) common variance.

Table 7: Parameter estimates of the latent class linear mixed model (3.4) with $g = 2$ mixture components, as well as under H_0 (of no random slope for Time^2)

		$d_{ii} \geq 0, \sigma^2 \geq 0$			Under $H_0 : d_{13} = d_{23} = d_{33} = 0, \sigma^2 \geq 0$		
Effect	Parameter	**Estimate**	**St. error**	p**-value**	**Estimate**	**St. Error**	p**-value**
Intercept	β_0	-0.0008	0.0148	0.9571	-0.0046	0.0193	0.8134
Time class 1	β_1^1	-0.0376	0.0633	0.5524	-0.2942	0.0664	<0.0001
Time class 2	β_1^2	-0.4498	0.0728	<0.0001	0.1417	0.1401	0.3118
Time^2 class 1	β_2^1	0.2351	0.1678	0.1612	1.3606	0.1705	<0.0001
Time^2 class 2	β_2^2	2.0801	0.1956	<0.0001	-0.5958	0.4031	0.1394
Time^3 class 1	β_3^1	-0.0556	0.1167	0.6339	-0.9709	0.1133	<0.0001
Time^3 class 2	β_3^2	-1.5250	0.1322	<0.0001	0.7284	0.2828	0.0100
Gender	β_4	-0.0058	0.0098	0.5538	-0.0111	0.0135	0.4119
Gender × Time	β_5	0.0672	0.0307	0.0288	0.0803	0.0356	0.0240
Group	β_6	0.0016	0.0062	0.7930	-0.0014	0.0082	0.8616
CMV	β_7	0.0021	0.0062	0.7356	0.0028	0.0079	0.7273
Age	β_8	0.0001	0.0003	0.7014	0.0003	0.0004	0.4825
var(b_{0i})	d_{11}	5.84×10^{-5}	–	–	1.53×10^{-5}	–	–
cov(b_{0i}, b_{1i})	d_{11}	-1.02×10^{-3}	–	–	-2.32×10^{-4}	–	–
var(b_{1i})	$d_{11} = d_{12}$	0.0196	–	–	0.0035	–	–
cov(b_{0i}, b_{2i})	$d_{13} = d_{31}$	1.50×10^{-3}	–		–	–	–
cov(b_{1i}, b_{2i})	$d_{23} = d_{32}$	-0.0261	–	–	–	–	–
var(b_{2i})	d_{33}	0.0384	–	–	–	–	–
Residual std. error	σ	0.0241	–	–	0.0346	–	–
-2×MLE	-512.26				-489.8		

Table 8: Latent class membership in two Latent classes

Class(C_i)	Latent class membership ID	Percentage (π_k)	Patients Distribution
1	2,3,4,8,9,10,11,12,13,14, 15,16,18,19,21,24,25,26, 27,28,29,31,34,40	60%	Gender(19 females, 5 males) Group (10 patients (0), 14 patients (1)) CMV (13 patients (0), 11 patients (1))
2	1,5,6,7,17,20,22,23, 30,32,33,35,36,37, 38,39	40%	Gender(15 females, 1 male) Group (10 patients (0), 6 patients (1)) CMV (7 patients (0), 9 patients (1))

3.3.1.1 Model Diagnostic

Model diagnostic plot is depicted in Figure A31. The Q-Q plot of patient-specific residuals is an almost straight line that indicates the assumption of normality is satisfied. The predicted individual and mean profiles are displayed in Figure A33 and Figure A34, respectively. These plots mimic observed plots and indicate the model is good for predicting the observed values. The correlation plot between observed and predicted $PIE63$ is displayed in Figure A36 and the correlation coefficient is 0.981. This indicates that there is high linear relationship between observed and predicted values.

3.3.1.2 Sensitivity Analysis

To explore the impact of deviations from the MAR assumption on the conclusions of the previous results, sensitivity analysis based on multiple imputations under MNAR via PMM approach with different scenarios was conducted. After imputing values, the parameter estimates are presented in Table A8. It is noticed that some parameter estimates

with their standard errors are similar with results under MAR provided in Table 7 and some are different. It indicates some results are sensitive when the MAR assumption fails, but it is not possible to test the MAR or MNAR assumption perfectly because of unknown missing values. Therefore, the estimated results should be interpreted with cautions.

3.3.2 Modeling of PIE63 for IL-2 Population

The linear mixed model (2.2) and latent class mixed model (2.4) with g mixture components were initially considered for modeling $PIE63$ for IL-2 population. Based on model comparison criteria and goodness-of-fits (described in Table A9), the final model (3.5) for kth latent class with $g = 3$ mixture components was chosen. The final model is defined as follows:

$$PIE63_{ij} = \beta_0 + b_{0i} + (\beta_1^k + b_{1i})Time_{ij} + \beta_2^k Time_{ij}^2 + \beta_3^k Time_{ij}^3 + \beta_4 Gender_i + \beta_5 Group_i + \beta_6 CMV_i + \beta_7 Age_i + \epsilon_{ij} \quad (3.5)$$

where $\boldsymbol{\beta} = (\beta_0, \beta_4, \beta_5, \beta_6, \beta_7, \beta_8)^t$ is the vector of overall fixed effects and $\boldsymbol{\delta}_k = (\beta_1^k, \beta_2^k, \beta_3^k,)^t$ is the kth class specific fixed effects. The $\boldsymbol{b}_{1i} = b_{0i}$ and $\boldsymbol{b}_{2i} = b_{1i}$ are the vector of patient specific random effects. The assumption of random effect $\boldsymbol{b}_{1i} \sim N(0, \boldsymbol{D}_{b_1})$ and $\boldsymbol{b}_{2i} \sim \sum_{k=1}^{g=2} \pi_k N(\boldsymbol{\mu}_k, \boldsymbol{D}_{b_2})$ with $\boldsymbol{\mu}_k = \mu_1^k$ are considered. The vectors $\boldsymbol{b}_i$, $i = 1, ..., 40$ are assumed to be independent. All error components ϵ_{ij} are assumed to be independent and normally distributed with mean zero and common variance σ^2. The significance of random slopes were checked and both slopes were found to be significant at 5% level. Therefore, they were retained in the model. The parameter estimates of model (3.5) are presented in the Table 9. It is observed that the covariates $gender$, $group$, CMV status and age were not significant.

Table 9: Parameter estimates of the latent class linear mixed model (3.5) with $g = 3$ mixture components, as well as under H_0 (of no random slope for Time) for modeling PIE63 of IL-2 T-cell Population

		$d_{ii} \geq 0, \sigma^2 \geq 0$			Under $H_0 : d_{12} = d_{21} = d_{22} = 0, \sigma^2 \geq 0$		
Effect	Parameter	**Estimate**	**St. error**	p-**value**	**Estimate**	**St. Error**	p-**value**
Intercept	β_0	0.0029	0.0049	0.5496	-0.0009	0.0051	0.8672
Time class1	β_1^1	-0.3164	0.0416	<0.0001	-0.3134	0.0510	0.0000
Time class2	β_1^2	-0.0296	0.0190	0.1198	-0.0278	0.0230	0.2277
Time class3	β_1^3	0.0998	0.0371	0.0071	0.1017	0.0453	0.0246
Time^2 class1	β_2^1	1.3215	0.1168	<0.0001	1.3169	0.1430	<0.0001
Time^2 class2	β_2^2	0.0815	0.0498	0.1016	0.0817	0.0604	0.1761
Time^2 class3	β_2^3	-0.5104	0.1042	<0.0001	-0.5157	0.1267	0.0001
Time^3 class1	β_3^1	-0.9759	0.0787	<0.0001	-0.9735	0.0966	<0.0001
Time^3 class2	β_3^2	-0.0458	0.0331	0.1665	-0.0473	0.0401	0.2384
Time^3 class3	β_3^3	0.5301	0.0703	<0.0001	0.5328	0.0855	<0.0001
Gender	β_4	-0.0003	0.0027	0.9033	0.0016	0.0029	0.5755
Group	β_5	0.0018	0.0020	0.3700	0.0023	0.0021	0.2609
CMV	β_6	0.0027	0.0019	0.1692	0.0049	0.0020	0.0131
Age	β_7	0.0000	0.0001	0.8348	0.0000	0.0001	0.8321
var(b_{0i})	d_{11}	6.32×10^{-6}	–	–	1.03×10^{-20}	–	–
cov(b_{0i}, b_{1i})	$d_{11} = d_{22}$	-3.36×10^{-5}	–	–	–	–	–
var(b_{1i})	d_{22}	0.0002	–	–	–	–	–
Residual st. error	σ	0.0091	–	–	0.0111	–	–
-2×MLE		-803.44			-786		

Based on posterior probabilities obtained by equation (2.5), patients are classified into three mixture classes. It is noticed that mixture class 1 contained 10% ($\pi_1 = 0.10$), class 2 contained 77.5% ($\pi_2 = 0.775$) and class 3 contained

12.5% ($\pi_3 = 0.125$) patients. Patient distribution of different latent classes is presented in Table 10. To get more insight about the reasons of this mixture, the association between latent class variable (C_i) and *sampling time* as well as *last exposure to VZV* were investigated. The results are presented in Table A11. It is observed that the $p-$value (chi-square = 15.03, p-value = 0.058) for testing the association between C_i and *sampling time* was on a borderline situation. Therefore, we can not get a concrete conclusion about this association. However,the strong association ($\eta = 0.776$) between C_i and *last exposure to VZV* was found. Both variables shared 60% (= η^2) common variance.

Table 10: Latent class membership in three Latent classes

Class(C_i)	Latent class membership ID	Percentage (π_k)	Patients Distribution
1	6,7,19,20	10%	Gender(4 females,0 males) Group (0=4 patient, 0 patients) CMV (0=2 patients, 1=2 patients)
2	4,5,8,9,10,12,13,14,15,16,17, 18,22,23,24,25,26,27,28,29,30, 31,32,33,34,35,36,37,38,39,40	77.50%	Gender(26 females, 5 male) Group (0=14 patients, 17 patients) CMV (0=15 patients, 1=16 patients)
3	1,2,3,11,21	12.50%	Gender(4 females,1 males) Group (2=10 patients, 3 patients) CMV (0=3 patients, 1=2 patients)

3.3.2.1 Model Diagnostic

Model diagnostic plots are presented in Figure A35. The Q-Q plot and histogram of patient specific residuals indicate the assumption of normality is satisfied. The predicted individual and mean profile are displayed in Figure 5 and Figure 6, respectively. Both plots indicate the model is good for predicting the observed values. The correlation between observed and predicted $PIE63$ is 0.956 which indicates, the predicted values are highly correlated with observed values.

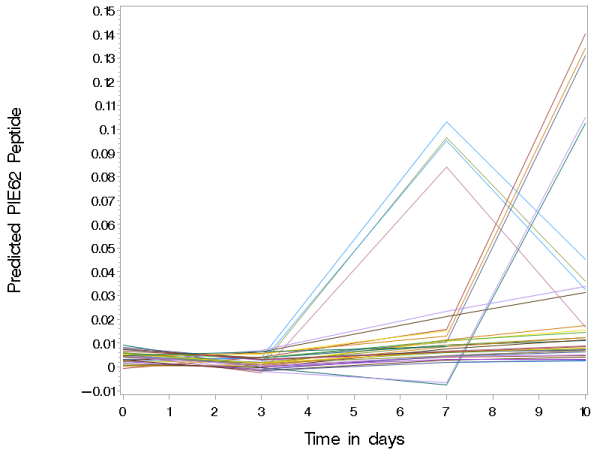

Figure 5: Predicted profile plots of PIE63 for IL-2

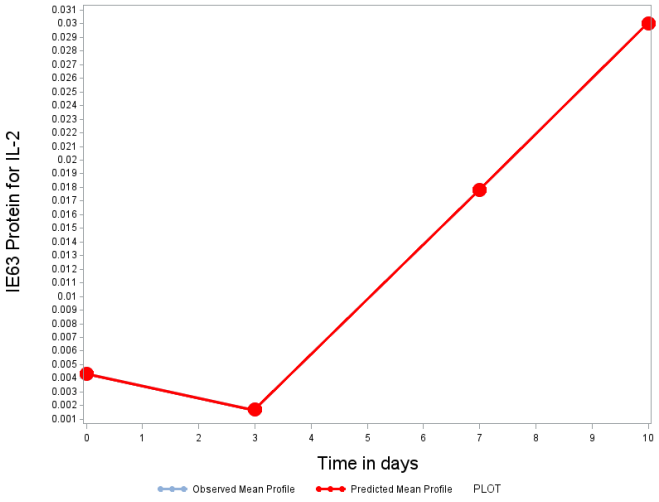

Figure 6: Observed and Predicted Mean Structure of PIE63 for IL-2

3.3.2.2 Sensitivity Analysis

The sensitivity analysis based on multiple imputation under MNAR assumption via PMM approach was conducted for the checking how robust the results are. The parameter estimation with different scenarios are displayed in Table A10.

It is observed that the estimated parameters under MNAR assumption are similar to the results under the assumption MAR which indicates the results are not sensitive.

3.3.3 Modeling of PIE63 for both IFN-γ and IL-2 Population

For describing the evolution of $PIE63$ for both IFN-γ and IL-2 population, the linear mixed model (2.2) and latent class linear mixed model (2.4) were considered initially. After model comparisons, the mixture mixed model (3.6) with $g = 2$ mixture components was chosen. Model comparison statistics are presented in Table A12. The selected model for kth latent class is given as:

$$PIE63_{ij} = \beta_0 + b_{0i} + (\beta_1^k + b_{1i})LogTime_{ij} + (\beta_2^k + b_{2i})LogTime_{ij}^2 + \beta_3^k LogTime_{ij}^3 + \beta_4 Gender_i + \beta_5 Group_i + \beta_6 CMV_i + \beta_7 Age_i + \epsilon_{ij} \quad (3.6)$$

where the usual notation $\boldsymbol{\beta} = (\beta_0, \beta_4, \beta_5, \beta_6, \beta_7, \beta_8)^t$ is the vector of overall fixed effects and $\boldsymbol{\delta}_k = (\beta_1^k, \beta_2^k, \beta_3^k,)^t$ is the kth class specific fixed effects. The $\boldsymbol{b}_{1i} = b_{0i}$ and $\boldsymbol{b}_{2i} = (b_{1i}, b_{2i})^t$ are the vector of patient-specific random effects. The assumption of random effect $\boldsymbol{b}_{1i} \sim N(0, \boldsymbol{D}_{b_1})$ and $\boldsymbol{b}_{2i} \sim \sum_{k=1}^{g=2} \pi_k N(\boldsymbol{\mu}_k, \boldsymbol{D}_{b_2})$ with $\boldsymbol{\mu}_k = (\mu_1^k, \mu_2^k)^t$ are made. The vectors $\boldsymbol{b}_i$, $i = 1, ..., 40$ are assumed to be independent. All error components ϵ_{ij} are assumed to be independent and normally distributed with mean zero and common variance σ^2. The significance of random slopes were checked and it was observed that both slopes were statistically significant at 5% level. The parameter estimates are tabulated in Table 11. It is seen that the evolution of $PIE63$ for the patients included in latent class 1 did not depend on time. This was also revealed in the observed profile plot shown in Figure A7. The evolution of $PIE63$ for patients included in latent class 2 depend on linear, quadratic and cubic actual time on logarithmic scale. It is also clearly seen that the covariates $gender$, $group$, CMV and age were not significant.

Table 11: Parameter estimates of the latent class linear mixed model (3.6) with $g = 2$ mixture components, as well as under H_0 (of no random slope for Time^2) for modeling PIE63 for both IFN-γ and IL-2 population

		$d_{ii} \geq 0, \sigma^2 \geq 0$			Under $H_0 : d_{13} = d_{23} = d_{33} = 0, \sigma^2 \geq 0$		
Effect	Parameter	**Estimate**	**St. error**	p-**value**	**Estimate**	**St. Error**	p-**value**
Intercept	β_0	0.0001	0.0033	0.9712	-0.0029	0.0047	0.5319
logTime class1	β_1^1	-0.0079	0.0094	0.3984	-0.0197	0.0172	0.252
logTime class2	β_1^2	-0.2844	0.0392	<0.0001	-0.0183	0.0315	0.5605
logTime^2 class1	β_2^1	0.0064	0.0100	0.5183	0.0211	0.0183	0.2501
logTime^2 class2	β_2^2	0.3146	0.0426	<0.0001	0.0146	0.0347	0.673
logTime^3 class1	β_3^1	-0.0008	0.0026	0.7552	-0.0052	0.0048	0.2767
logTime^3 class2	β_3^2	-0.0797	0.0111	<0.0001	-0.0013	0.0091	0.8903
Gender	β_4	0.0003	0.0018	0.8587	0.0035	0.0024	0.1416
Group	β_5	0.0001	0.0013	0.9915	-0.0006	0.0018	0.7486
CMV	β_6	-0.0007	0.0013	0.5680	-0.0003	0.0017	0.8742
Age	β_7	0.0001	0.0001	0.4810	0.0001	0.0001	0.2836
var(b_{0i})	d_{11}	4.14×10^{-8}	–	–	2.85×10^{-19}	–	–
cov(b_{0i}, b_{1i})	$d_{12} = d_{21}$	1.21×10^{-6}	–	–	-5.23×10^{-19}	–	–
var(b_{1i})	d_{22}	3.49×10^{-5}	–	–	9.67×10^{-19}	–	–
cov(b_{0i}, b_{2i})	$d_{13} = d_{31}$	-8.02×10^{-7}	–	–	–	–	–
cov(b_{1i}, b_{2i})	$d_{23} = d_{32}$	-2.33×10^{-5}	–	–	–	–	–
var(b_{2i})	d_{33}	1.55×10^{-5}	–	–	–	–	–
Residual st. error	σ	0.0040	–	–	0.0063	–	–
-2×MLE		-596.74			-561.8		

The latent class factor (C_i) with its membership patient ID and patient allocation in other factor covariates are presented

in Table 12. Patients are classified into two mixture classes based on posterior probabilities. The latent class 1 contained 77.14% patients and class 2 contained remaining 22.86% patients. To investigate the reasons of this mixture, the association between latent class variable (C_i) and *sampling time* as well as *last exposure to VZV* were scrutinized. The results are tabulated in Table A11. The results show that there was a strong association (chi-square = 10.90, p-value = 0.028) between C_i and *sampling time*. It is also noticed that there was a strong association ($\eta = 0.748$) between C_i and *last exposure to VZV*. Both variables shared 56% (= η^2) common variance.

Table 12: Latent class membership in two Latent classes

Class(C_i)	Latent class membership ID	Percentage (π_k)	Patients Distribution
1	4,5,9,10,12,13,14,15,16,17 18,19,20,22,24,25,26,28,30, 32,33,34,35,36,37,38,39	77.14%	Gender(23 females,4 males) Group (0=14 patients, 13 patients) CMV (13=2 patients, 1=14 patients)
2	1,2,3,6,7, 11,21,23	22.86%	Gender(7 females, 1 male) Group (0=4 patients, 4 patients) CMV (0=4 patients, 1=4 patients)

3.3.3.1 Model Diagnostic

Model diagnostic plots are presented in Figure A37. The Q-Q plot of patient-specific residuals indicates the assumption of normality seems to be met. The predicted individual and mean profiles are displayed in Figure 7 and Figure 8, respectively. Both plots indicate the model is good for predicting the observed values. The correlation between observed and predicted $PIE63$ is 0.941 which indicates, the predicted values are highly correlated with observed values.

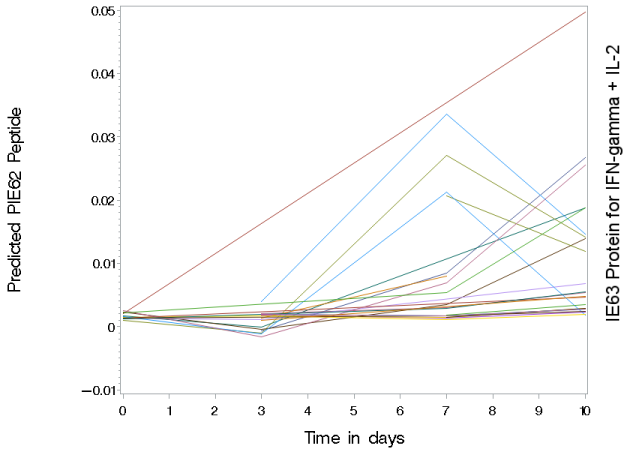

Figure 7: Predicted profile plots of PIE63 for both IFN-γ and IL-2

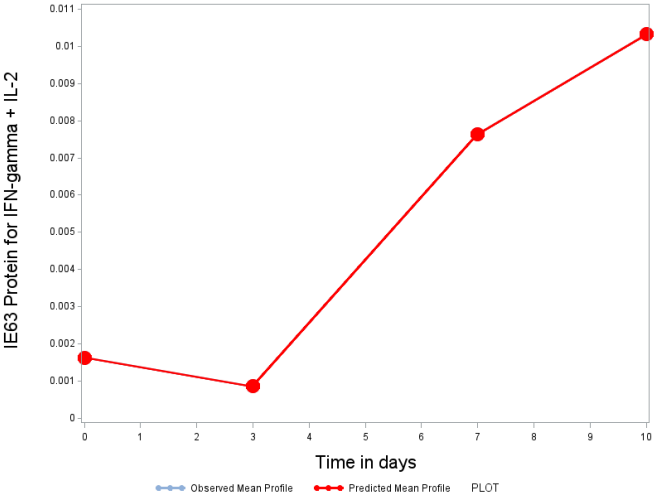

Figure 8: Observed and Predicted Mean Structure of PIE63 for both IFN-γ and IL-2

3.3.3.2 Sensitivity Analysis

The sensitivity analysis was performed to check how sensitive the parameter estimates are when the MAR assumption for missing mechanism is violated. Multiple imputations under MNAR assumption based on PMM approach with various scenarios were performed to impute missing values. After imputing values, parameter estimates with their standard errors are tabulated in Table A13. Most of the parameters estimates are not different from results obtained under MAR but some of the estimates are different. It means the results under MAR are a little bit sensitive. However, the p-value for testing hypothesis of each parameter under MNAR are very close to that of under MAR.

4 Discussion and Conclusions

The main objectives of this research were to study the evolution of T-cell proliferation over time following stimulation of antigen-specific IE62 and IE63 peptides in the different T-cells populations: IFN-γ, IL-2, and both IFN-γ and IL-2 and how these proliferation's depend on $gender$, Cytomegalovirus (CMV) status, $group$ status and age. The data were collected from the blood samples from 40 patients on the initial time (0), 3rd, 7th, and 10th day after applying antigen-specific IE62 and IE63 peptides based on vitro stimulation experiments. The response variables ($PIE62$ and $PIE62$) were measured based on the difference between the percentages of antigen stimulus-induced IFN-γ or/and IL-2-producing T-cell subtypes and the percentage from the unstimulated samples per stimulus. The data contained some missing values due to the nature of the study, missingness is expected as some patients may drop out from the study (Molenberghs and Kenward (2007); Little et al. (2012)). In this case missingness has to do with the experiment causing uninterpretable results.

From exploratory data analysis, it was seen that there was a lot of between and within variability in $PIE62$ and $PIE63$ score of patients in all T-cell populations. The mean plot of $PIE62$ over time indicates a slight linear increased of $PIE62$ for IFN-γ population. The curvature evolution was observed for IL-2, and both IFN-γ and IL-2 populations. On the other hand, the mean plot of $PIE63$ over time indicates the curvature evolution of $PIE63$ for all T-cell populations. The average evolution was also investigated by the each category of $gender$, $group$ and CMV status since it was useful in order to choose fixed effects for a mean structure of a mixed model. It was suggested to keep the interaction between $gender$ and $time$ in the model which could be an important factor in mean structure. Moreover, bivariate association between $gender$, $group$, and CVM were found not significant by using chi-square and Fisher exact tests. The age of the patients at entry in the study ranges from 22 to 53 years and the average age was 39.03 years.

The random-effects model was employed to study the T-cell proliferation and dynamic changes over time following stimulation of antigen-specific IE62 peptides for different T-cell populations. For IFN-γ population, the linear proliferation of T-cell was found to be significant and the significant effect of the interaction between $time$ and $gender$ was identified. Each patient had different proliferation rate over time. It was noticed that the T-cell proliferation for males was higher than that of females. The age of the patient, $group$ and CMV were not significant on the evolution of T-cell proliferation for IFN-γ population.

The LMM with patient-specific slopes of a linear and quadratic time was conducted for describing the T-cell proliferation and dynamic changes over time following stimulation of antigen-specific IE62 peptides for IL-2 T-cell population. The cubic proliferation of T-cell was found to be significant as well as the interaction between $gender$ and $time$. The covariates $group$, CMV and age were not significant on this proliferation of T-cell for IL-2 population.

For both IFN-γ and IL-2 T-cell population, the LMM with random slopes of linear and quadratic time was fitted to describe the T-cell proliferation over time following stimulation of antigen-specific IE62 peptides. The main effect of $gender$, quadratic $time$ and their interaction were significant on this proliferation. The covariate $group$ was significant. The NICU nurses group (0) had less T-cell proliferation rate than pediatric group (1). Again, other covariates CMV status and age were not significant on this T-cell proliferation for both IFN-γ and IL-2 population.

The latent class linear mixed model was fitted to describe the T-cell proliferation and dynamics change over time following stimulation of antigen-specific IE63 peptides all T-cell populations. For IFN-γ population, a LCMM with two mixture components was fitted. It was observed that the T-cell proliferation of patients included in class one depend on the interaction between $gender$ and $time$. On the other hand, the T-cell proliferation for patients included in latent class two depend on linear, quadratic and cubic time as well as interaction between $gender$ and $time$. Patients were classified into mixture classes based on their posterior probabilities. Class one contained 60% patients while class two contained remaining 20% patients. The covariates $group$, CMV status and age were not significant on the proliferation of T-cell for IFN-γ population.

The LCMM with three mixture components was fitted for describing T-cell proliferation following stimulation of

antigen-specific IE63 peptides for IL-2 population. Class one, two and three contained 10%, 77.5% and 12.5% patients, respectively. Cubic time was found to be significant for patients in class one and class three whereas for those class two it was not significant. The average T-cell proliferation for class one patient's decreased sharply after the 7th day while it increased rapidly in class three after the 7th day. There was no significant effect of $gender$, $group$, CMV and age on this proliferation.

Finally, the LCMM with two mixture components model was fitted to describe T-cell proliferation, for both IFN-γ and IL-2 population after using antigen specific IE63 peptides. Class one that consist of 77.14% of patients had evolution not depending on time. On the other hand, for patient included in class two there was a significant cubic effect of time on the proliferation of T-cells. It is worth noting that T-cell proliferation did not depend on covariates $gender$, $group$, CMV status and age in this population.

The possible reasons for the mixture of IE63 were investigated. The association between the latent class variable and the sampling time of patient allocation as well as the time since last exposure to VZV were found to be significant. Therefore, it can be concluded that the sampling time and the time since last exposure to VZV were possible reasons for building the mixture of IE63. And these variables are important in statistical point of view, although sampling time might not be important in biological point of view.

The likelihood-based analysis has been done under the MAR principle. Molenberghs et al. (2004) discussed the sense in which likelihood-based MAR methods are consistent with the ITT principle. To explore the impact of deviations from the assumption of MAR, sensitivity analysis was performed based on multiple imputations under the MNAR assumption with different scenarios, based on the PMM approach. Some conclusions are sensitive for violating the MAR assumption of missingness mechanism. However, some careful considerations have to be made, the most important one of which is that no modelling approach, whether either MAR or MNAR, can recover the lack of information that occurs due to incompleteness of the data (Molenberghs and Kenward; 2007).

This study has some limitations and concerns. There were some patients with intermittent missingness pattern, who did not get a lot of attention in order to see their actual impact on the results and the reason of absent measurements. In addition, other sensitivity analysis could be done, as a way to carefully check the assumptions of missing mechanism. Further studies, combining selection models and pattern-mixture models may also be an option (Molenberghs and Kenward; 2007). Local influence ideas can also be used as a sensitivity analysis tool. Further discussion about local influence can be found in Molenberghs et al. (2003), Shen et al. (2006), Molenberghs and Kenward (2007), Verbeke and Molenberghs (2000), and Molenberghs and Verbeke (2005).

References

Arvin, A., Gershon, A. and Calisher, C. (2001). *Immunity to and Prevention of Herpes Zoster*, Springer.

Baiker, A., Bagowski, C., Ito, H., Sommer, M., Zerboni, L., Fabel, K., Hay, J., Ruyechan, W. and Arvin, A. M. (2004). The immediate-early 63 protein of varicella-zoster virus: analysis of functional domains required for replication in vitro and for t-cell and skin tropism in the scidhu model in vivo, *Journal of virology* **78**(3): 1181–1194.

Belisle, S. E., Yin, J., Shedlock, D. J., Dai, A., Yan, J., Hirao, L., Kutzler, M. A., Lewis, M. G., Andersen, H., Lank, S. M. et al. (2011). Long-term programming of antigen-specific immunity from gene expression signatures in the pbmc of rhesus macaques immunized with an siv dna vaccine, *PLoS One* **6**(6): e19681.

Berger, R., Florent, G. and Just, M. (1981). Decrease of the lymphoproliferative response to varicella-zoster virus antigen in the aged., *Infection and Immunity* **32**(1): 24–27.

Campbell, J. J., Murphy, K. E., Kunkel, E. J., Brightling, C. E., Soler, D., Shen, Z., Boisvert, J., Greenberg, H. B., Vierra, M. A., Goodman, S. B. et al. (2001). Ccr7 expression and memory t cell diversity in humans, *The Journal of Immunology* **166**(2): 877–884.

Celeux, G., Lavergne, C. and Martin, O. (2002). Mixture of linear mixed models application to repeated data clustering.

Fitzmaurice, G., Laird, N. and Ware, J. (2004). *Applied Longitudinal Analysis*, Wiley Series in Probability and Statistics - Applied Probability and Statistics Section Series, Wiley.

Fiuza, J. A., Fujiwara, R. T., Gomes, J., Rocha, M., Chaves, A. T., de Araújo, F. F., Fares, R., Teixeira-Carvalho, A., Martins-Filho, O. d. A., Cancado, G. et al. (2009). Profile of central and effector memory t cells in the progression of chronic human chagas disease, *PLoS Negl Trop Dis* **3**(9): e512.

Flatt, A. and Breuer, J. (2012). Varicella vaccines, *British medical bulletin* p. lds019.

Frey, C. R., Sharp, M. A., Min, A. S., Schmid, D. S., Loparev, V. and Arvin, A. M. (2003). Identification of cd8+ t cell epitopes in the immediate early 62 protein (ie62) of varicella-zoster virus, and evaluation of frequency of cd8+ t cell response to ie62, by use of ie62 peptides after varicella vaccination, *Journal of Infectious Diseases* **188**(1): 40–52.

Gałecki, A. and Burzykowski, T. (2013). *Linear mixed-effects models using R: A step-by-step approach*, Springer Science & Business Media.

Hayward, A. (2001). *In vitro measurement of human T cell responses to varicella zoster virus antigen*, Springer.

Houseman, E. A., Ryan, L. M. and Coull, B. A. (2004). Cholesky residuals for assessing normal errors in a linear model with correlated outcomes, *Journal of the American Statistical Association* **99**(466): 383–394.

Jensen, W. A., Birch, J. B. and Woodall, W. H. (2006). Profile monitoring via linear mixed models, *Journal of Quality Technology (to appear, 2007)* .

Jones, L., Black, A. P., Malavige, G. N. and Ogg, G. S. (2007). Phenotypic analysis of human cd4+ t cells specific for immediate early 63 protein of varicella-zoster virus, *European journal of immunology* **37**(12): 3393–3403.

Laird, N. M. and Ware, J. H. (1982). Random-effects models for longitudinal data, *Biometrics* pp. 963–974.

Lanzavecchia, A. and Sallusto, F. (2000). Dynamics of t lymphocyte responses: intermediates, effectors, and memory cells, *Science* **290**(5489): 92–97.

Lenk, P. J. and DeSarbo, W. S. (2000). Bayesian inference for finite mixtures of generalized linear models with random effects, *Psychometrika* **65**(1): 93–119.

Levin, M. J., Smith, J. G., Kaufhold, R. M., Barber, D., Hayward, A. R., Chan, C. Y., Chan, I. S., Li, D. J., Wang, W., Keller, P. M. et al. (2003). Decline in varicella-zoster virus (vzv)–specific cell-mediated immunity with increasing age and boosting with a high-dose vzv vaccine, *Journal of Infectious Diseases* **188**(9): 1336–1344.

Little, R. J., D'Agostino, R., Cohen, M. L., Dickersin, K., Emerson, S. S., Farrar, J. T., Frangakis, C., Hogan, J. W., Molenberghs, G., Murphy, S. A. et al. (2012). The prevention and treatment of missing data in clinical trials, *New England Journal of Medicine* **367**(14): 1355–1360.

Little, R. J. and Rubin, D. B. (1989). The analysis of social science data with missing values, *Sociological Methods & Research* **18**(2-3): 292–326.

Malavige, G., Jones, L., Black, A. and Ogg, G. (2008). Varicella zoster virus glycoprotein e-specific cd4+ t cells show evidence of recent activation and effector differentiation, consistent with frequent exposure to replicative cycle antigens in healthy immune donors, *Clinical & Experimental Immunology* **152**(3): 522–531.

Miller, A. E. (1980). Selective decline in cellular immune response to varicella-zoster in the elderly, *Neurology* **30**(6): 582–582.

Molenberghs, G. and Kenward, M. (2007). *Missing data in clinical studies*, John Wiley & Sons.

Molenberghs, G., Thijs, H., Jansen, I., Beunckens, C., Kenward, M. G., Mallinckrodt, C. and Carroll, R. J. (2004). Analyzing incomplete longitudinal clinical trial data, *Biostatistics* **5**(3): 445–464.

Molenberghs, G., Thijs, H., Kenward, M. G. and Verbeke, G. (2003). Sensitivity analysis of continuous incomplete longitudinal outcomes, *Statistica Neerlandica* **57**(1): 112–135.

Molenberghs, G. and Verbeke, G. (2005). *Models for Discrete Longitudinal Data*, Springer Series in Statistics, Springer New York.

Muthén, B. and Shedden, K. (1999). Finite mixture modeling with mixture outcomes using the em algorithm, *Biometrics* pp. 463–469.

Ogunjimi, B., Smits, E., Hens, N., Hens, A., Lenders, K., Ieven, M., Van Tendeloo, V., Van Damme, P. and Beutels, P. (2011). Exploring the impact of exposure to primary varicella in children on varicella-zoster virus immunity of parents, *Viral immunology* **24**(2): 151–157.

Ogunjimi, B., Smits, E., Heynderickx, S., Van den Bergh, J., Bilcke, J., Jansens, H., Malfait, R., Ramet, J., Maecker, H. T., Cools, N. et al. (2014b). Influence of frequent infectious exposures on general and varicella-zoster virus-specific immune responses in pediatricians, *Clinical and Vaccine Immunology* **21**(3): 417–426.

Ogunjimi, B., Theeten, H., Hens, N. and Beutels, P. (2014a). Serology indicates cytomegalovirus infection is associated with varicella-zoster virus reactivation, *Journal of medical virology* **86**(5): 812–819.

Proust, C. and Jacqmin-Gadda, H. (2005). Estimation of linear mixed models with a mixture of distribution for the random effects, *Computer methods and programs in biomedicine* **78**(2): 165–173.

Proust-Lima, C., Philipps, V. and Liquet, B. (2015). Estimation of extended mixed models using latent classes and latent processes: the r package lcmm, *arXiv preprint arXiv:1503.00890* .

Sadzot-Delvaux, C. and Rentier, B. (2001). *The role of varicella zoster virus immediate-early proteins in latency and their potential use as components of vaccines*, Springer.

Sallusto, F., Geginat, J. and Lanzavecchia, A. (2004). Central memory and effector memory t cell subsets: function, generation, and maintenance, *Annu. Rev. Immunol.* **22**: 745–763.

Schafer, J. L. (1997). *Analysis of incomplete multivariate data*, CRC press.

Shen, S., Beunckens, C., Mallinckrodt, C. and Molenberghs, G. (2006). A local influence sensitivity analysis for incomplete longitudinal depression data, *Journal of biopharmaceutical statistics* **16**(3): 365–384.

Spengler, M., Niesen, N., Grose, C., Ruyechan, W. and Hay, J. (2001). *Interactions among structural proteins of varicella zoster virus*, Springer.

Steain, M., Sutherland, J. P., Rodriguez, M., Cunningham, A. L., Slobedman, B. and Abendroth, A. (2014). Analysis of t cell responses during active varicella-zoster virus reactivation in human ganglia, *Journal of virology* **88**(5): 2704–2716.

Tan, F. E., Ouwens, M. J. and Berger, M. P. (2001). Detection of influential observations in longitudinal mixed effects regression models, *Journal of the Royal Statistical Society: Series D (The Statistician)* **50**(3): 271–284.

Verbeke, G. and Lesaffre, E. (1996). A linear mixed-effects model with heterogeneity in the random-effects population, *Journal of the American Statistical Association* **91**(433): 217–221.

Verbeke, G. and Molenberghs, G. (2000). *Linear Mixed Models for Longitudinal Data*, Springer Series in Statistics, Springer New York.

Yuan, Y. (2014). Sensitivity analysis in multiple imputation for missing data, *Proceedings of the SAS Global Forum 2014 Conference:[http://support. sas. com/resources/papers/proceedings14/SAS270-2014. pdf]*.

Zerboni, L. and Arvin, A. (2015). Neuronal subtype and satellite cell tropism are determinants of varicella-zoster virus virulence in human dorsal root ganglia xenografts in vivo, *PLoS Pathog* **11**(6): e1004989.

This page intentionally left blank

5 Appendix

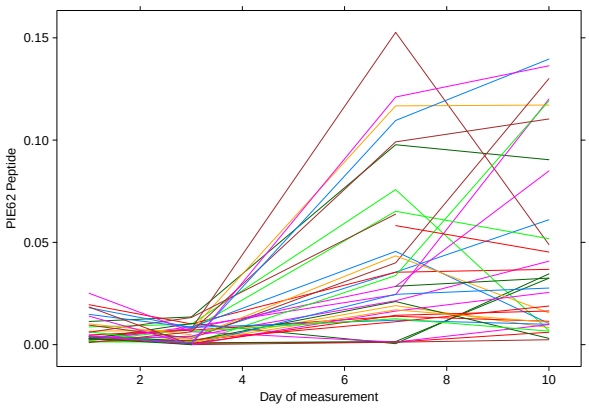

Figure A1: Individual profile plots of PIE62 for IL-2

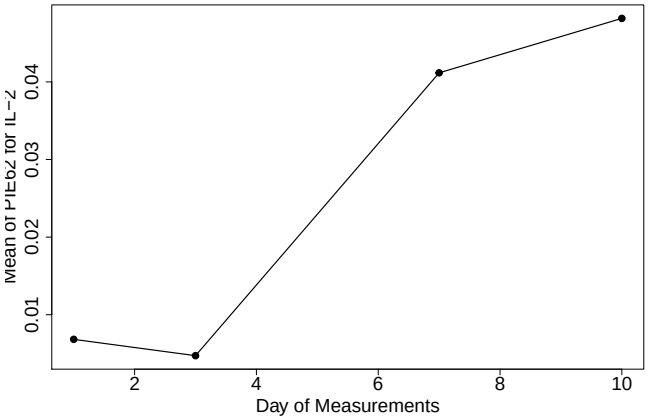

Figure A2: Mean Structure of of PIE62 for IL-2

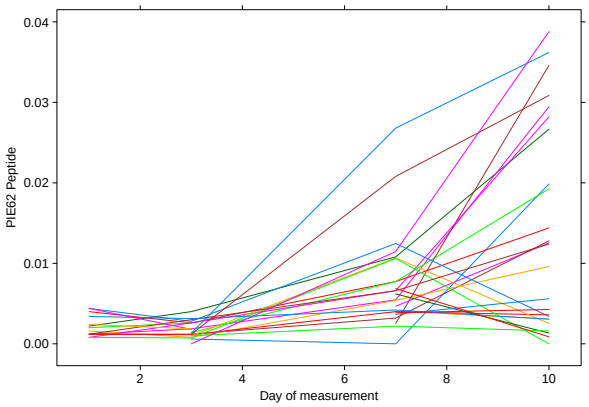

Figure A3: Individual profile plots of PIE62 for both IFN-γ and IL-2

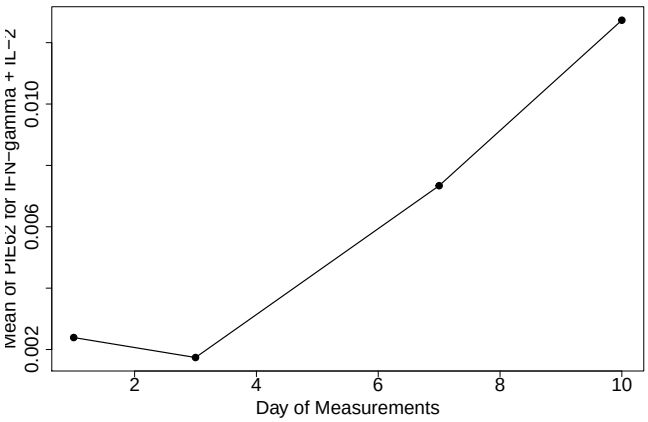

Figure A4: Mean Structure of PIE62 for both IFN-γ and IL-2

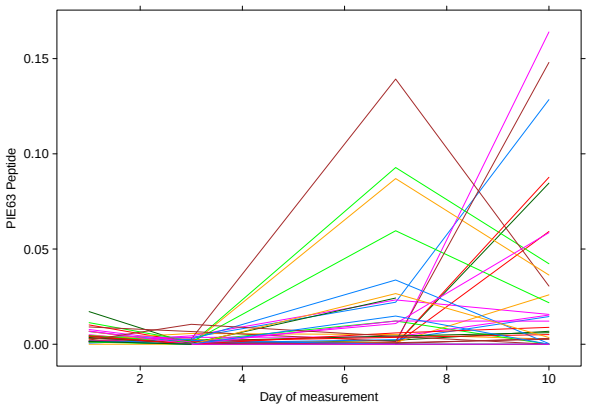

Figure A5: Individual profile plots of PIE63 for IL-2

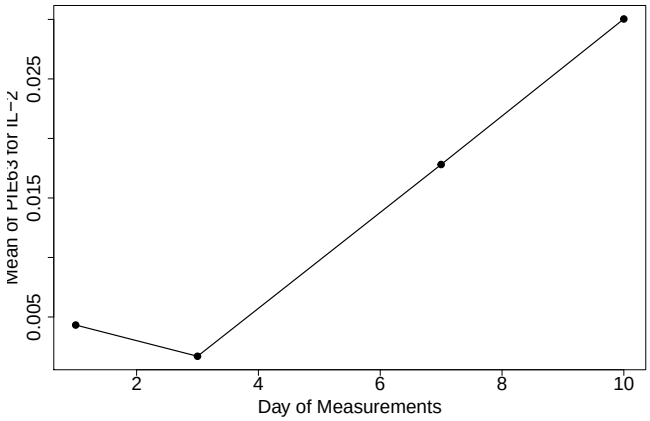

Figure A6: Mean Structure of PIE63 for IL-2

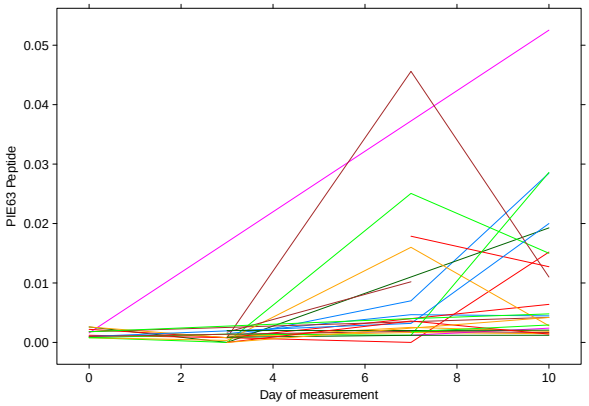

Figure A7: Individual profile plots of PIE63 for both IFN-γ and IL-2

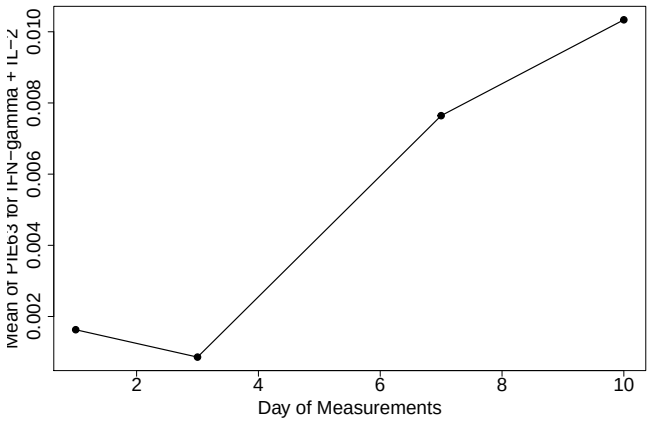

Figure A8: Mean Structure of PIE63 for both IFN-γ and IL-2

Table A1: Correlation Matrix of PIE62 over different time for different T-cell populations (output categories)

	IFN-γ				**IL-2**				**IFN-γ and IL-2**			
-	**Day 0**	**Day 3**	**Day 7**	**Day 10**	**Day 0**	**Day 3**	**Day 7**	**Day 10**	**Day 0**	**Day 3**	**Day 7**	**Day 10**
Day 0	1.000	0.487*	-0.212	-0.091	1.000	0.204	-0.203	-0.267	1.000	0.365	0.307	-0.147
Day 3	0.487*	1.000	-0.065	0.075	0.204	1.000	0.263	0.024	0.365	1.000	-0.011	-0.038
Day 7	-0.212	-0.065	1.000	0.293	-0.203	0.263	1.000	0.596*	0.307	-0.011	1.000	0.419*
Day 10	-0.091	0.075	0.293	1.000	-0.267	0.024	0.596*	1.000	-0.147	-0.038	0.419*	1.000

"*" = Significant at 5% level

Table A2: Correlation Matrix of PIE63 over different time for different T-cell populations (output categories)

	IFN-γ				**IL-2**				**IFN-γ and IL-2**			
	Day 0	**Day 3**	**Day 7**	**Day 10**	**Day 0**	**Day 3**	**Day 7**	**Day 10**	**Day 0**	**Day 3**	**Day 7**	**Day 10**
Day 0	1.000	0.445*	-0.049	0.458*	1.000	-0.118	-0.257	0.364	1.000	-0.118	-0.475	-0.056
Day 3	0.445*	1.000	0.299	0.187	-0.118	1.000	-0.082	0.106	-0.118	1.000	-0.309	-0.022
Day 7	-0.049	0.299	1.000	0.020	-0.257	-0.082	1.000	-0.019	-0.475	-0.309	1.000	0.154
Day 10	0.458*	0.187	0.020	1.000	0.364	0.106	-0.019	1.000	-0.056	-0.022	0.154	1.000

"*" = Significant at 5% level

Table A3: Investigating the association between categorical covariates

Nominal variable-1	Nominal variable-2	Fisher exact Test (p-value)	Chi-square (p-value)	Conclusion
Gender	Group	0.1199	0.0765	No Association
Gender	CMV	0.9900	0.9900	No Association
Group	CMV	0.2683	0.0765	No Association

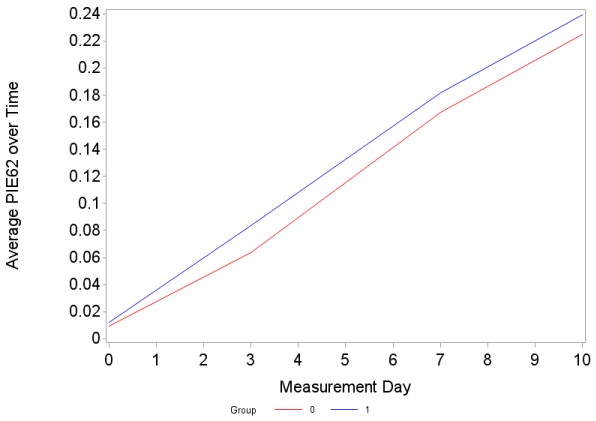

Figure A9: Mean plots of PIE62 by Group for IFN-γ

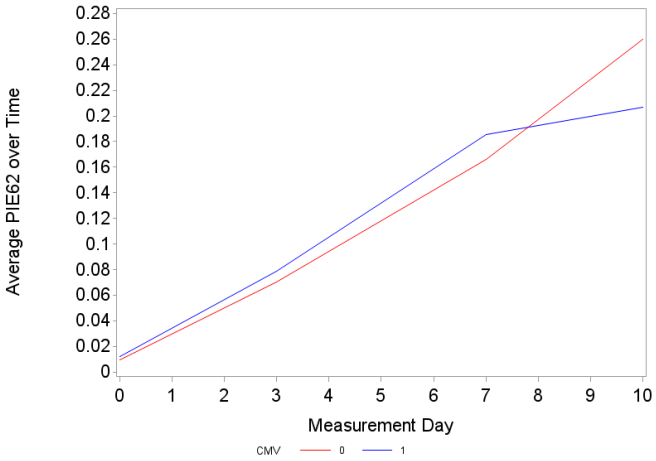

Figure A10: Mean plots of PIE62 by CMV for IFN-γ

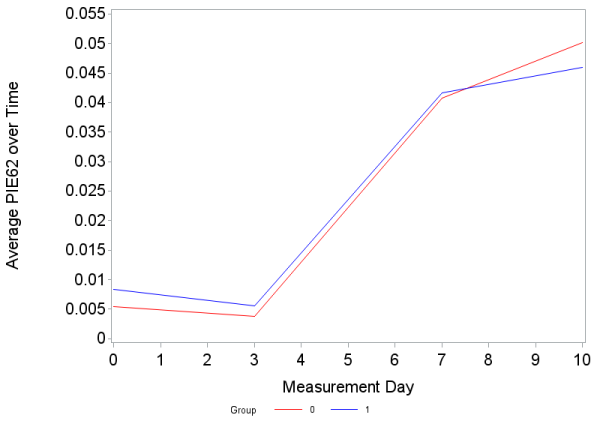

Figure A11: Mean plots of PIE62 by Group for IL-2

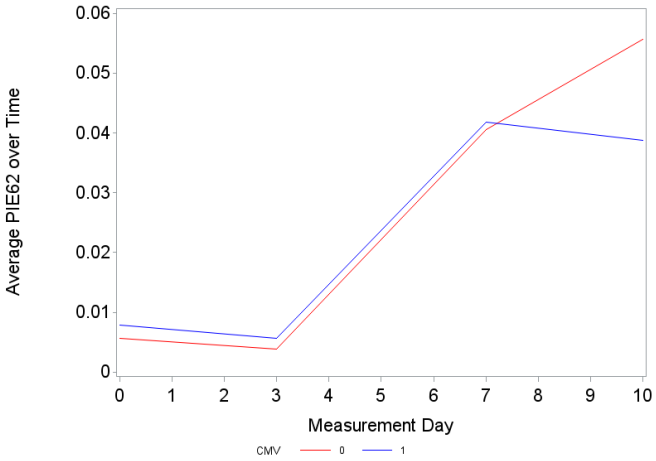

Figure A12: Mean plots of PIE62 by CMV for IL-2

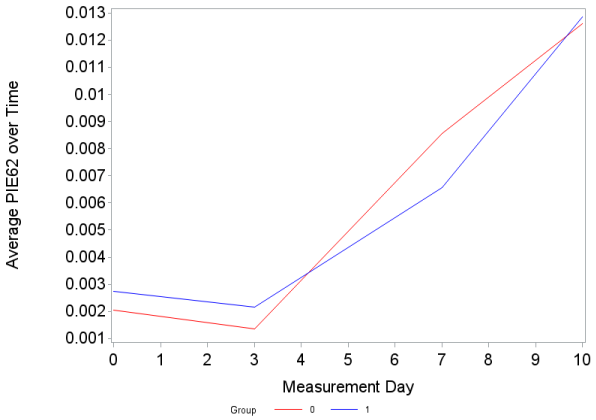

Figure A13: Mean plots of PIE62 by Group for both IFN-γ and IL-2 population

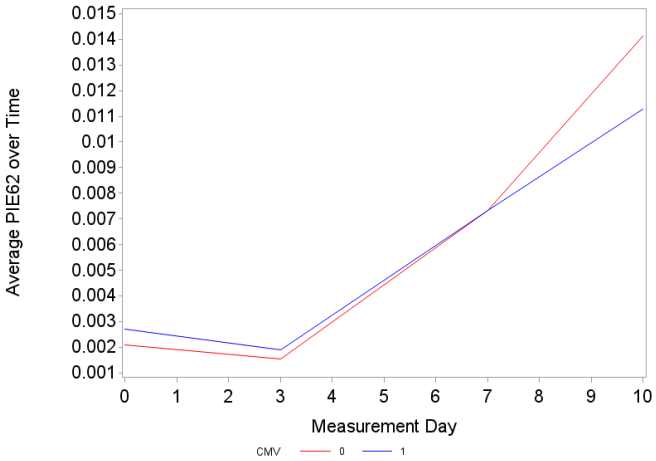

Figure A14: Mean plots of PIE62 by CMV for both IFN-γ and IL-2 population

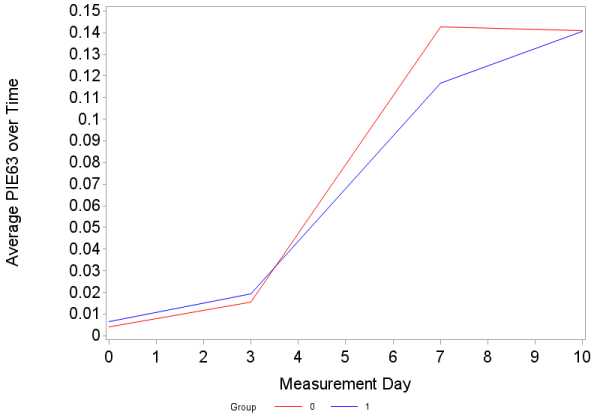

Figure A15: Mean plots of PIE63 by Group for IFN-γ

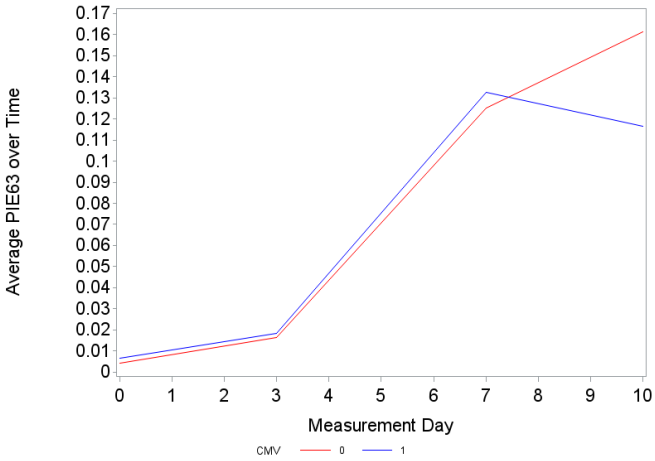

Figure A16: Mean plots of PIE63 by CMV for IFN-γ

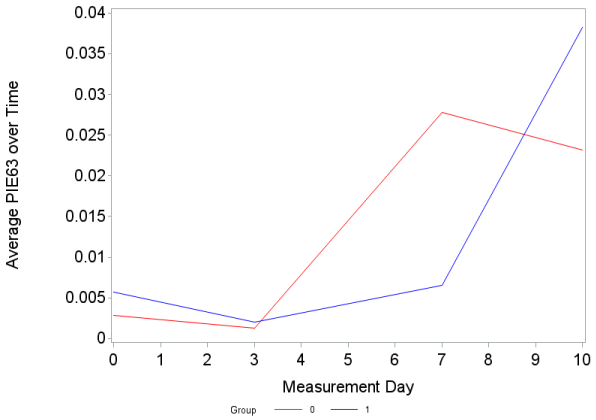

Figure A17: Mean plots of PIE63 by Group for IL-2

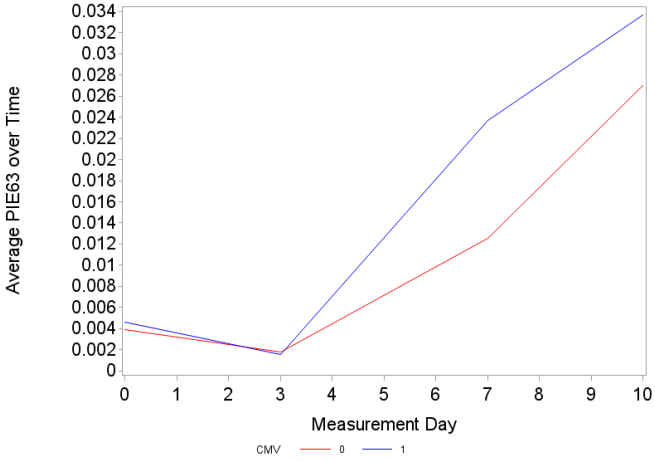

Figure A18: Mean plots of PIE63 by CMV for IL-2

Table A4: LMM parameter estimation per dropout pattern

		Pattern 1			**Pattern 2**		
Effect	**Parameter**	**Estimate**	**Standard**	p**-value**	**Estimate**	**Standard**	p**-value**
Intercept	β_0	0.0075	0.0335	0.8277	-0.0409	0.0397	0.3334
Time	β_1	0.3627	0.1395	0.0220	0.3602	0.0445	$<$0.0001
Gender	β_2	0.0367	0.0307	0.2500	0.0206	0.0195	0.2999
Gender$\times$Time	β_3	-0.1804	0.1445	0.2312	-0.1132	0.0484	0.0274
Group	β_4	-0.0218	0.0099	0.0429	-0.0134	0.0131	0.3179
CMV	β_5	-0.0139	0.0102	0.1950	-0.0067	0.0174	0.7048
Age	β_6	-0.0003	0.0005	0.5815	0.0006	0.0010	0.5329

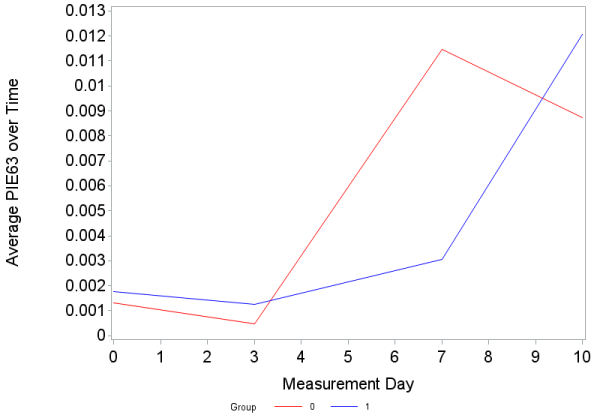

Figure A19: Mean plots of PIE63 by Group for both IFN-γ and IL-2 population

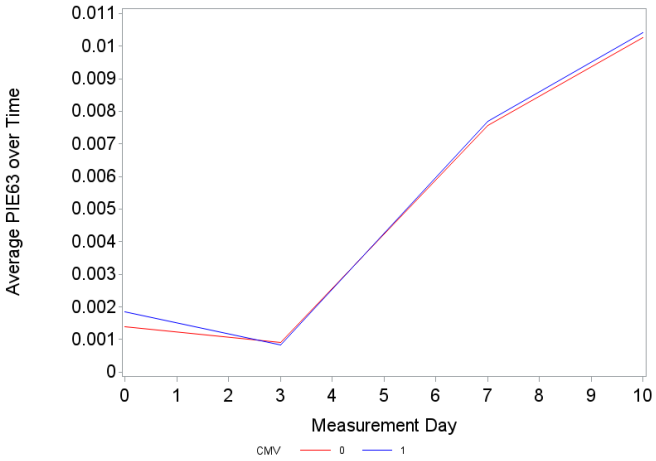

Figure A20: Mean plots of PIE63 by CMV for both IFN-γ and IL-2 population

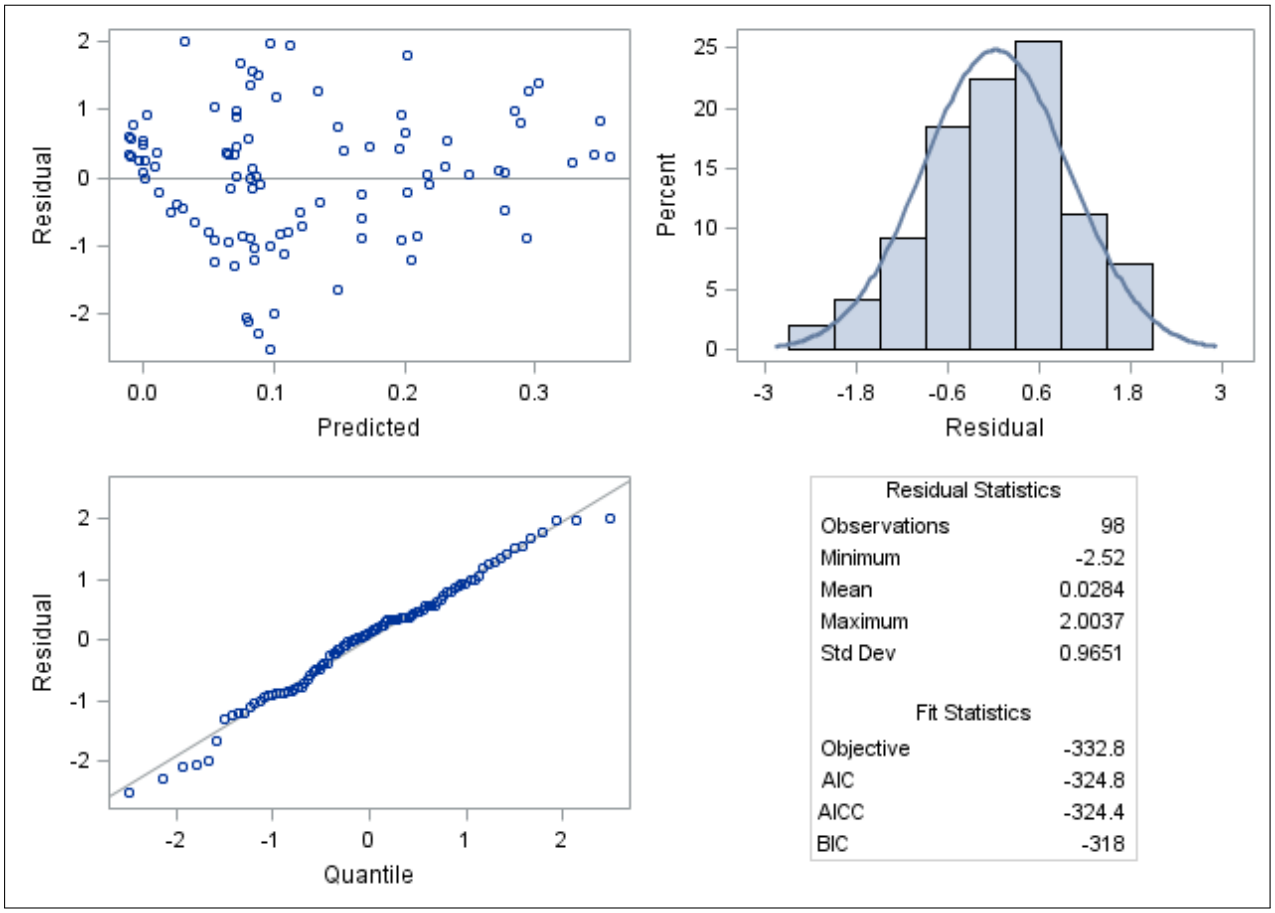

Figure A21: Diagnostic plots of model (3.1) of PIE62 for IFN-γ

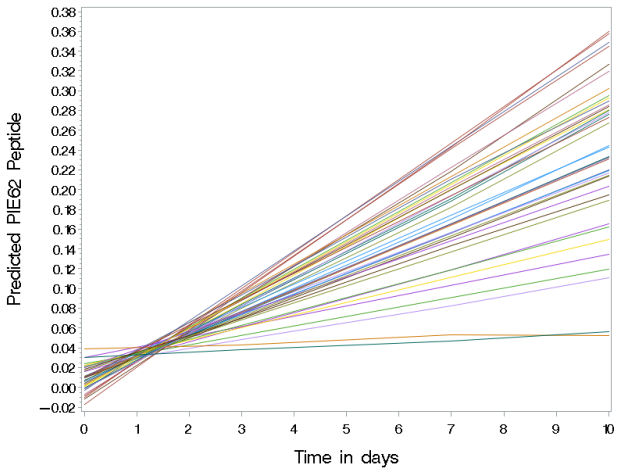

Figure A22: Predicted profile plots of PIE62 for IFN-γ

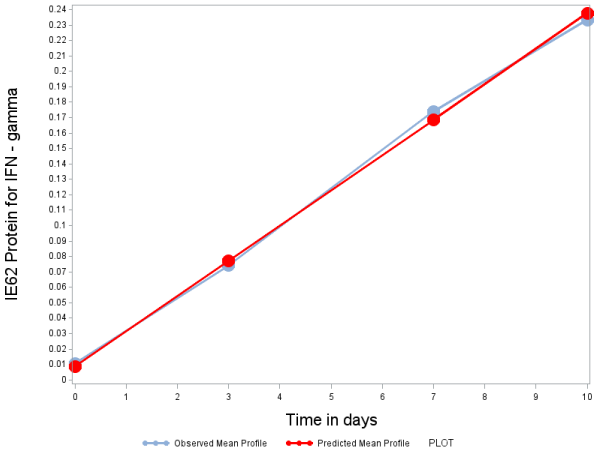

Figure A23: Observed and Predicted Mean Structure of PIE62 for IFN-γ

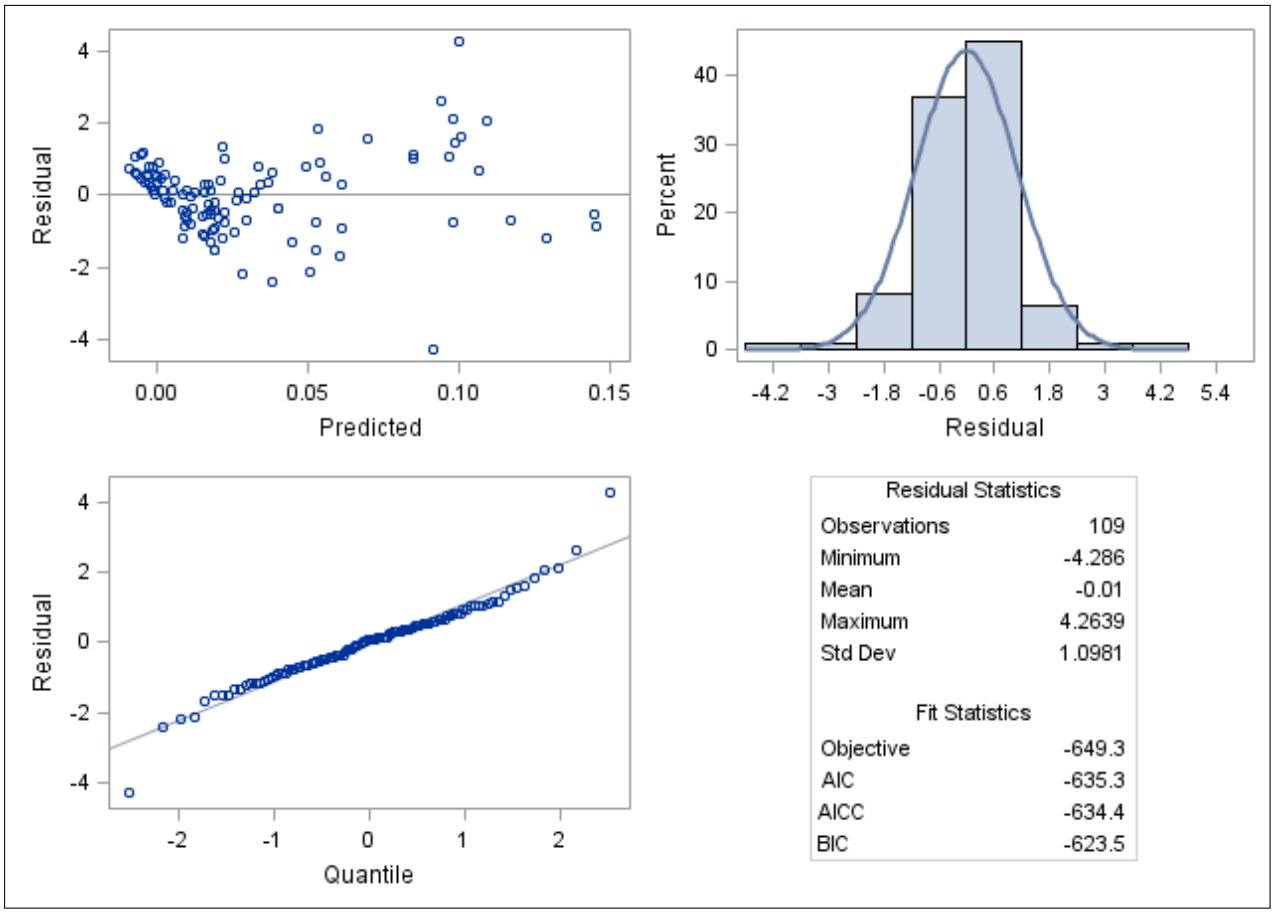

Figure A24: Diagnostic plots of model (3.2) of PIE62 for IL-2

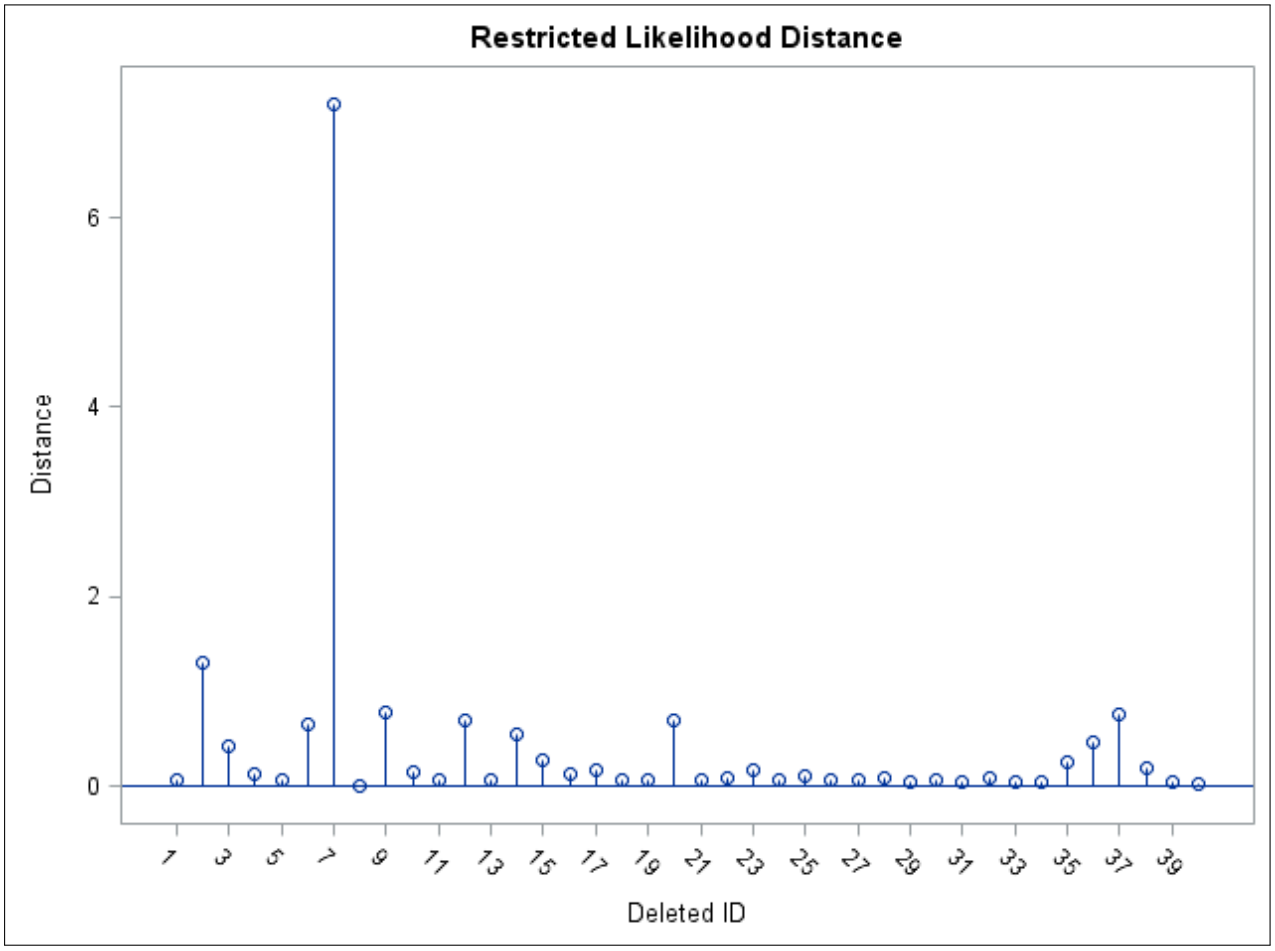

Figure A25: Global influence plot by using model (3.2) of PIE62 for IL-2

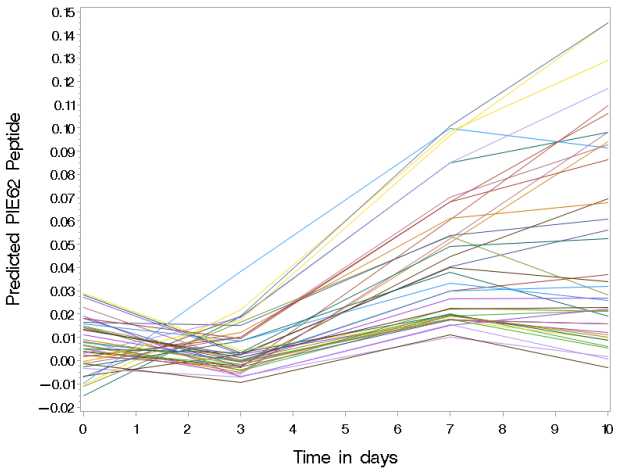

Figure A26: Predicted profile plots of PIE62 for IL-2

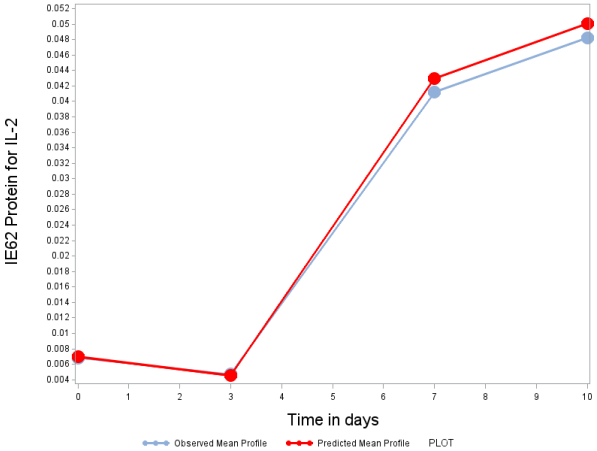

Figure A27: Observed and Predicted Mean Structure of PIE62 for IL-2

Table A5: Sensitivity analysis of LMM (3.2) under different scenarios by using multiple imputation (imputed 10 data sets)

		PMM under MNAR			
		Shift = 0.10		Shift = 0.20	
Effect	Parameter	Estimate	Std. Error	Estimate	Std. Error
Intercept	β_0	0.0102	0.0176	0.0199	0.0310
Time	β_1	-0.0578	0.0674	-0.0733	0.1074
Time^2	β_2	0.4217	0.1550	0.4435	0.2522
Time^3	β_3	-0.2559	0.1024	-0.2625	0.1659
Gender	β_4	0.0287	0.0136	0.0441	0.0236
Gender×Time	β_5	-0.0840	0.0301	-0.0931	0.0404
Group	β_6	-0.0028	0.0064	-0.0070	0.0111
CMV	β_7	0.0032	0.0063	0.0023	0.0108
Age	β_8	-0.0004	0.0004	-0.0006	0.0006

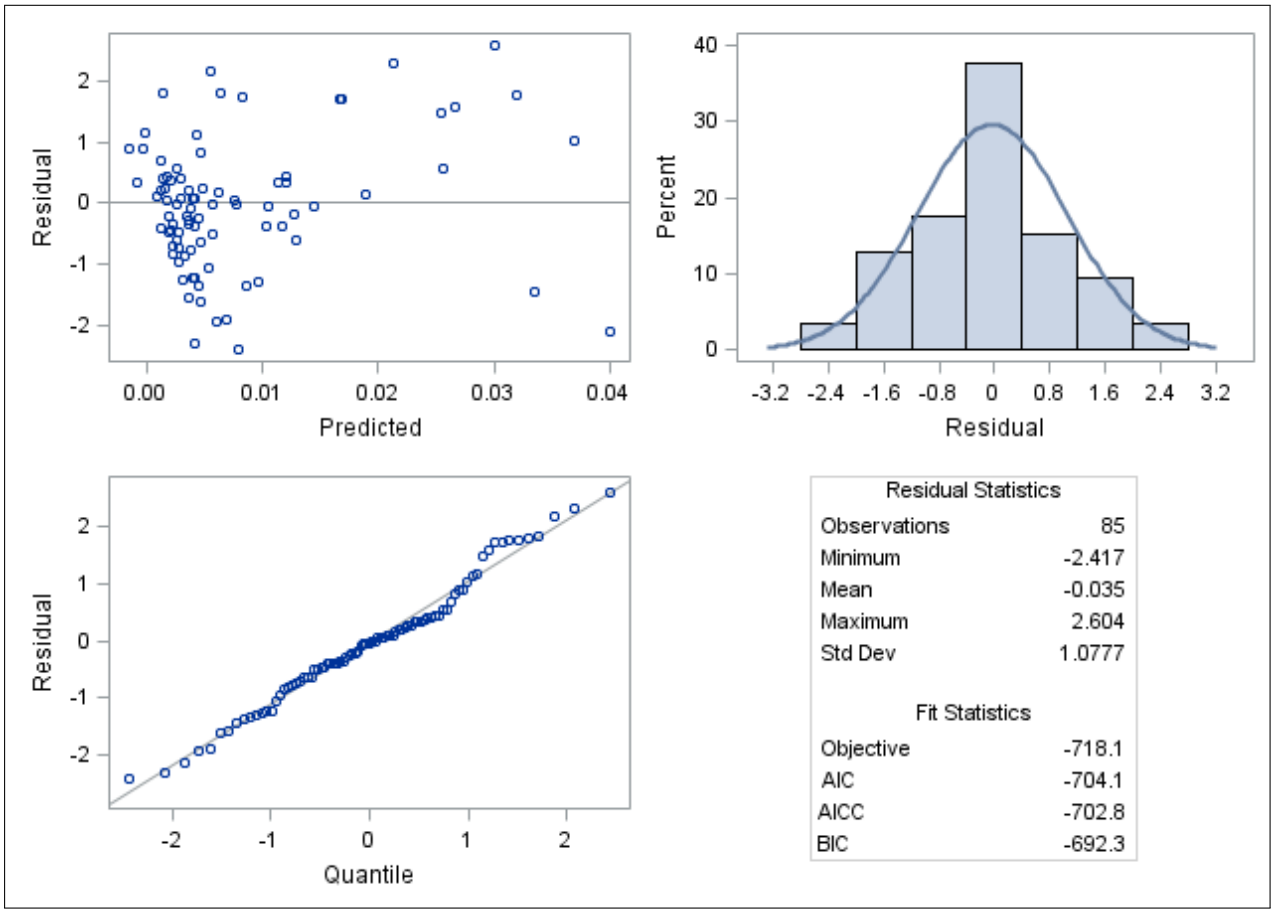

Figure A28: Diagnostic plots of model (3.3) of PIE62 for both IFN-γ and IL-2

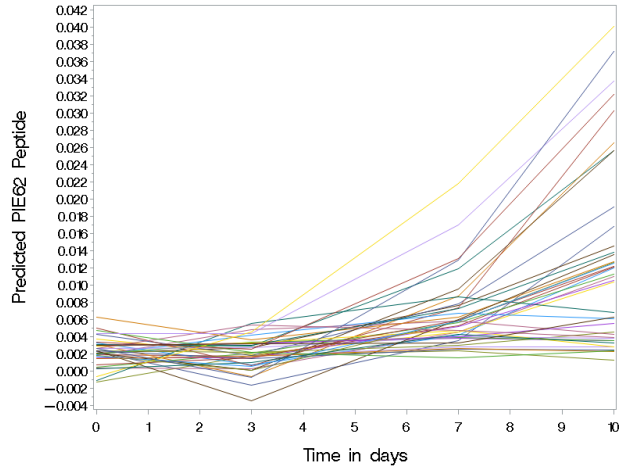

Figure A29: Predicted profile plots of PIE62 for IFN-γ and IL-2

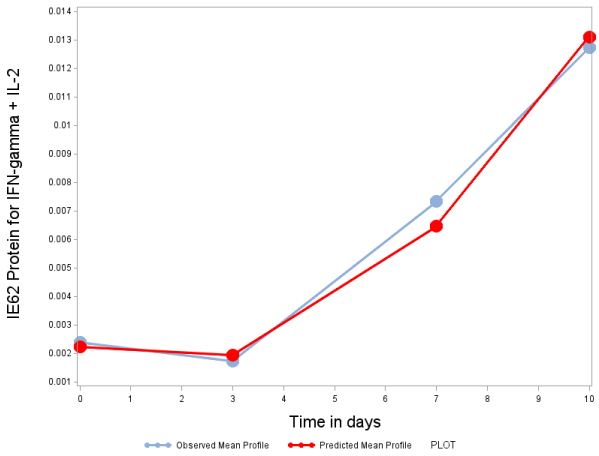

Figure A30: Observed and Predicted Mean Structure of PIE62 for both IFN-γ and IL-2

Table A6: Sensitivity analysis for linear mixed model (3.3) under three different scenarios by using multiple imputation (10 imputed data sets)

		PMM under MNAR			
		Shift=0.10		Shift=0.20	
Effect	Parameter	Estimate	Std. Error	Estimate	Std. Error
Intercept	β_0	0.0061	0.0233	0.0065	0.0459
Time	β_1	0.0016	0.0308	-0.0017	0.0602
Time^2	β_2	0.0166	0.0323	0.0194	0.0616
Gender	β_3	0.0466	0.0170	0.0944	0.0336
Time$^2\times$ Gender	β_4	-0.0395	0.0207	-0.0708	0.0390
Group	β_5	0.0032	0.0089	0.0053	0.0175
CMV	β_6	0.0088	0.0087	0.0157	0.0170
Age	β_7	-0.0002	0.0005	-0.0004	0.0009

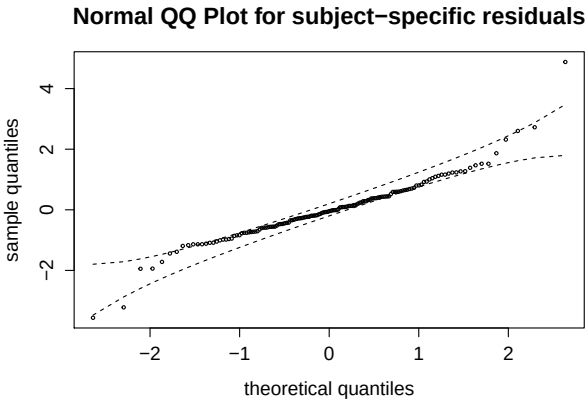

Figure A31: Diagnostics plots of model (3.4) of PIE63 for IFN-γ

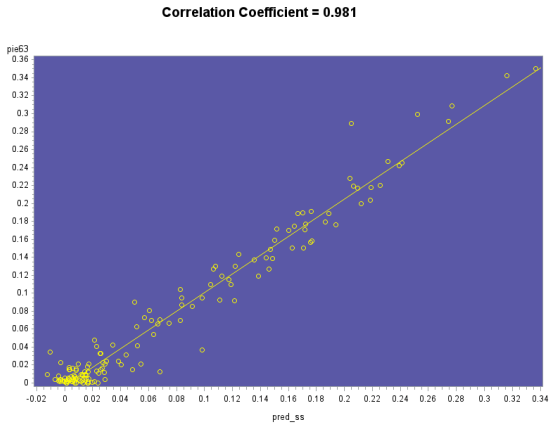

Figure A32: Correlation plot of Predicted by using (3.4) and Observed PIE63 for IFN-γ Population

Table A7: Choosing the best model by comparison of different models for IFN-γ Population

SL	Model	Random Effect	g	MLE	AIC	Diagnostics
1	Time, Time^2, Time^3, Gender, Gender$\times$Time, Group, CMV, Age	Intercept	1	210.43	-398.87	Not good
2	Time, Time^2, Time^3, Gender, Gender$\times$Time, Group, CMV, Age	Intercept , Time	1	220.46	-414.93	Not good
3	Time, Time^2, Time^3, Gender, Gender$\times$Time, Group, CMV, Age	Intercept, Time, Time^2	1	230.11	-428.22	Not good
4	Time, Time^2, Time^3, Gender, Gender$\times$Time, Group, CMV, Age	Intercept	2	210.50	-395.00	Not good
5	Time, Time^2, Time^3, Gender, Gender$\times$Time, Group, CMV, Age	Intercept , Time	2	221.75	-411.49	Not good
6	Time, Time^2, Time^3, Gender, Gender$\times$Time, Group, CMV, Age	Intercept, Time, Time^2	2	231.74	-423.49	Not good
7	Time, Time^2, Time^3, Gender, Gender$\times$Time, Group, CMV, Age (with mixture Time^3)	Intercept, Time, Time^2	2	256.13	-472.27	Good

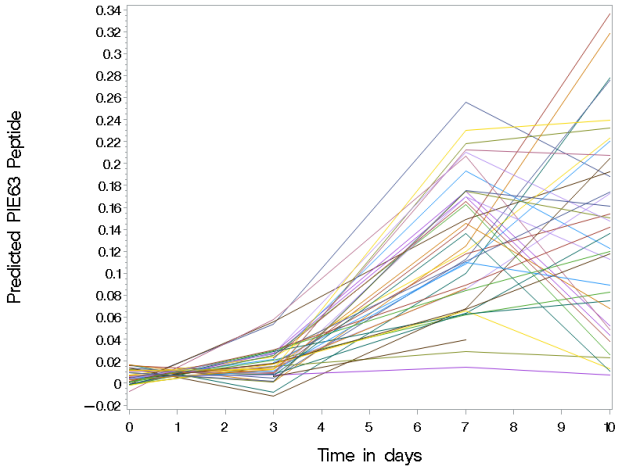

Figure A33: Predicted profile plots of PIE63 for IFN-γ

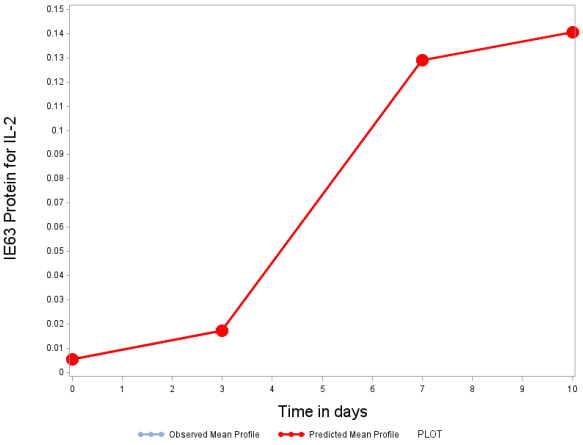

Figure A34: Observed and Predicted Mean Structure of PIE63 for IFN-γ

Table A8: Sensitivity analysis of LCMM (3.4) under different scenarios by using multiple imputation (imputed 10 data sets)

		PMM under MNAR			
		Shift = 0.10		Shift = 0.20	
Effect	Parameter	Estimate	Std. Error	Estimate	Std. Error
Intercept	β_0	-0.00502	0.01714	0.01666	0.02078
Time class 1	β_1^1	-0.03171	0.07352	-0.19898	0.07841
Time class 2	β_1^2	-0.45572	0.09234	-0.67197	0.12856
Time^2 class 1	β_2^1	0.23760	0.20885	0.65551	0.19439
Time^2 class 2	β_2^2	2.09459	0.26893	2.82138	0.38436
Time^3 class 1	β_3^1	-0.06686	0.14679	-0.33242	0.12917
Time^3 class 2	β_3^2	-1.54067	0.18922	-2.10634	0.28634
Gender	β_4	-0.00364	0.01157	-0.02561	0.01900
Gender $\times$ Time	β_5	0.09154	0.03265	0.11862	0.04541
Group	β_6	0.00171	0.00710	-0.00897	0.00792
CMV	β_7	0.00851	0.00691	0.00993	0.00765
Age	β_8	0.00016	0.00038	0.00021	0.00044

Table A9: Choosing the best model by comparison of different models for IL-2 Population

SL	Fixed Effect	Random Effect	g	value of ML	AIC	Diagnostic
1	Time, Time^2, Time^3, Group, Gender, CMV, Age	Intercept, Time	1	311.57	-599.13	not good
2	Time, Time^2, Time^3, Group, Gender, CMV, Age	Int., Time, Time^2	1	322.83	-615.66	not good
3	Time, Time^2, Time^3, Group, Gender, CMV, Age	Intercept, Time	2	311.57	-593.13	not good
4	Time, Time^2, Time3, Group, Gender, CMV, Age	Int., Time, Time^2	2	333.07	-628.13	not good
5	Time, Time^2, Time^3, Group, Gender, CMV, Age	Intercept, Time	3	319.82	-603.64	not good
6	Time, Time^2 (also mixture) , Group, Gender, CMV, Age	Intercept, Time	3	347.62	-657.27	not good
7	Time, Time^2, Time^3 (mixture),	Intercept, Time	3	401.72	-763.43	good

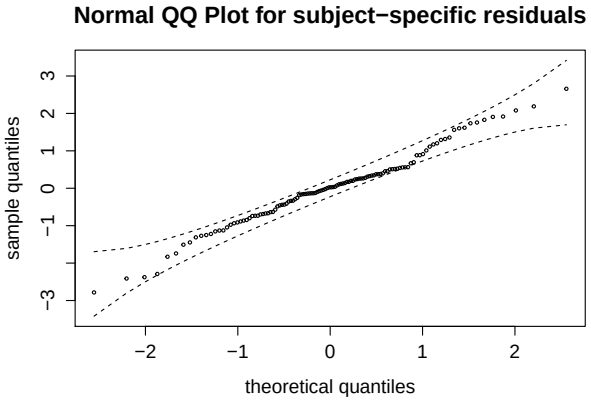

Figure A35: Diagnostics plots of model (3.5) of PIE63 for IL-2

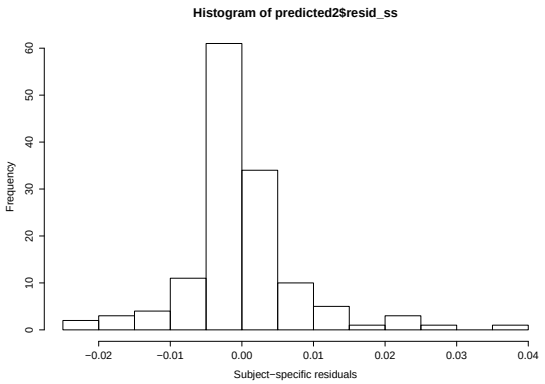

Figure A36: Histogram of patient-specific residuals

Table A10: Sensitivity analysis of latent class linear mixed model (3.5) under different scenarios by using multiple imputation (imputed 10 data sets)

		PMM under MNAR			
		Shift = 0.10		Shift = 0.20	
Effect	Parameter	Estimate	Std. Error	Estimate	Std. Error
Intercept	β_0	-0.0006	0.0066	0.0005	0.0063
Time class1	β_1^1	-0.3021	0.0665	-0.2581	0.0604
Time class2	β_1^2	-0.0187	0.0281	-0.0396	0.0252
Time class3	β_1^3	0.0922	0.0584	0.1004	0.0530
Time^2 class1	β_2^1	1.2698	0.1925	0.9676	0.1757
Time^2 class2	β_2^2	0.0624	0.0748	0.1353	0.0668
Time^2 class3	β_2^3	-0.4637	0.1610	-0.4955	0.1496
Time^3 class1	β_3^1	-0.9334	0.1308	-0.7460	0.1198
Time^3 class2	β_3^2	-0.0370	0.0499	-0.0894	0.0446
Time^3 class3	β_3^3	0.4833	0.1071	0.5054	0.1023
Gender	β_4	0.0033	0.0037	0.0007	0.0035
Group	β_5	0.0005	0.0027	0.0004	0.0025
CMV	β_6	0.0041	0.0027	0.0029	0.0025
Age	β_7	0.0001	0.0001	0.0001	0.0001

Table A11: Association between latent class variable (C_i) and sampling time as well as last exposure to VZV

Population	C_i	Variables	**Statistic**	**Value**	**Prob**
IFN-γ	C_i	Sampling Time	Chi-Square	10.833	0.0285
		Last exposure to VZV	Eta (η)	0.5200	
IL-2	C_i	Sampling Time	Chi-Square	15.0323	0.0585
		Last exposure to VZV	Eta (η)	0.7760	
IFN-γ and IL-2	C_i	Sampling Time	Chi-Square	10.8970	0.0277
		Last exposure to VZV	Eta (η)	0.7480	

Table A12: Choosing the best model by comparison of different models for both IFN-γ and IL-2 Population

SL	Model	Random Effect	g	MLE	AIC	Diagnostics
1	LTime, LTime^2, LTime^3, Group, Gender, CMV, Age	int, LTime	1	275.49	-526.98	not good
2	LTime, LTime^2, LTime3, Group, Gender, CMV, Age	int, LTime, LTime^2	1	278.39	-526.78	not good
3	LTime, LTime^2, LTime^3, Group, Gender, CMV, Age	int, LTime	2	275.49	-520.98	not good
4	LTime, LTime^2, LTime^3, Group, Gender, CMV, Age	int, LTime, LTime^2	2	278.39	-518.78	not good
5	LTime, LTime^2, LTime^3(mixture), Group, Gender, CMV, Age	int, LTime, LTime^2	2	298.38	-556.76	good
6	LTime, LTime^2, LTime^3(mixture), Group, Gender, CMV, Age	int (no mix.), LTime, LTime^2	2	298.37	-558.73	good

N. B. LTime=Log(Time)

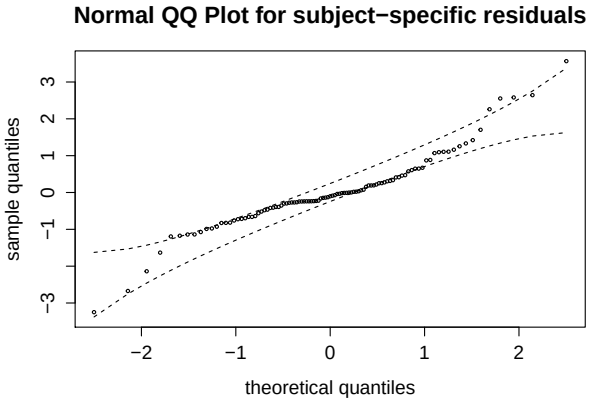

Figure A37: Diagnostics plots of model (3.6) of PIE63 for both IFN-γ and IL-2

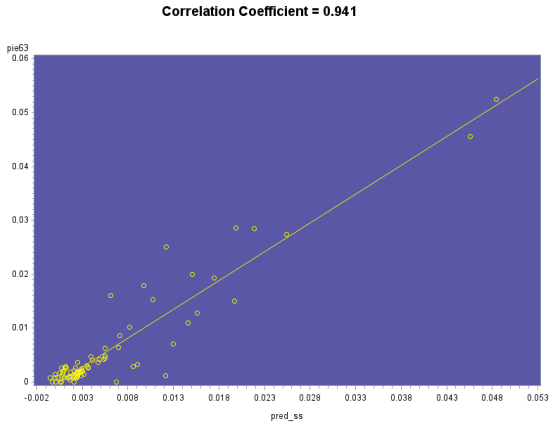

Figure A38: Correlation plot of Predicted by using (3.6) and Observed PIE63 for both IFN-γ and IL-2 Population

Table A13: Sensitivity analysis of latent class linear mixed model (3.6) under different scenarios by using multiple imputation (imputed 10 data sets)

		PMM under MNAR			
		Shift = 0.10		Shift = 0.20	
Effect	Parameter	Estimate	Std. Error	Estimate	Std. Error
Intercept	β_0	-0.0090	0.0086	-0.0012	0.0126
logTime class1	β_1^1	-0.0068	0.0211	-0.0313	0.0291
logTime class2	β_1^2	-0.1764	0.0645	-0.3091	0.0935
logTime^2 class1	β_2^1	0.0020	0.0217	0.0206	0.0285
logTime^2 class2	β_2^2	0.2535	0.0679	0.4356	0.0949
logTime^3 class1	β_3^1	-0.0026	0.0056	-0.0093	0.0073
logTime^3 class2	β_3^2	-0.0672	0.0177	-0.1175	0.0245
Gender	β_4	0.0066	0.0050	0.0092	0.0062
Group	β_5	-0.0050	0.0032	-0.0055	0.0043
CMV	β_6	0.0056	0.0032	0.0031	0.0042
Age	β_7	0.0004	0.0002	0.0004	0.0002

Auteursrechtelijke overeenkomst

Ik/wij verlenen het wereldwijde auteursrecht voor de ingediende eindverhandeling:
Longitudinal modeling of T-cell dynamics during in vitro stimulation experiments

Richting: **Master of Statistics-Biostatistics**
Jaar: **2015**

in alle mogelijke mediaformaten, - bestaande en in de toekomst te ontwikkelen - , aan de Universiteit Hasselt.

Niet tegenstaand deze toekenning van het auteursrecht aan de Universiteit Hasselt behoud ik als auteur het recht om de eindverhandeling, - in zijn geheel of gedeeltelijk -, vrij te reproduceren, (her)publiceren of distribueren zonder de toelating te moeten verkrijgen van de Universiteit Hasselt.

Ik bevestig dat de eindverhandeling mijn origineel werk is, en dat ik het recht heb om de rechten te verlenen die in deze overeenkomst worden beschreven. Ik verklaar tevens dat de eindverhandeling, naar mijn weten, het auteursrecht van anderen niet overtreedt.

Ik verklaar tevens dat ik voor het materiaal in de eindverhandeling dat beschermd wordt door het auteursrecht, de nodige toelatingen heb verkregen zodat ik deze ook aan de Universiteit Hasselt kan overdragen en dat dit duidelijk in de tekst en inhoud van de eindverhandeling werd genotificeerd.

Universiteit Hasselt zal mij als auteur(s) van de eindverhandeling identificeren en zal geen wijzigingen aanbrengen aan de eindverhandeling, uitgezonderd deze toegelaten door deze overeenkomst.

Voor akkoord,

Karim, Md. Rezaul

Datum: **1/09/2015**